THESIS FOR THE DEGREE OF LICENTIATE ENGINEERING

Towards Topography Characterization of Additive Manufacturing Surfaces

AMOGH VEDANTHA KRISHNA

Department of Industrial and Materials Science
Chalmers University of Technology
Gothenburg, Sweden 2020

Towards topography characterization of additive manufacturing surfaces
AMOGH VEDANTHA KRISHNA

Thesis for the degree of Licentiate of Engineering

Report no. IMS-2020-8

Published and distributed by:
Department of Industrial and Materials Science
Chalmers University of Technology
SE - 412 96 Gothenburg, Sweden

Printed in Sweden
Chalmers Digitaltryck
Gothenburg, Sweden 2020

Telephone + 46 (0)31-772 1000

Towards topography characterization of additive manufacturing surfaces
AMOGH VEDANTHA KRISHNA
Department of Industrial and Materials Science
Chalmers University of Technology

ABSTRACT

Additive Manufacturing (AM) is on the verge of causing a downfall to conventional manufacturing with its huge potential in part manufacture. With an increase in demand for customized product, on-demand production and sustainable manufacturing, AM is gaining a great deal of attention from different industries in recent years. AM is redefining product design by revolutionizing how products are made. AM is extensively utilized in automotive, aerospace, medical and dental applications for its ability to produce intricate and lightweight structures. Despite their popularity, AM has not fully replaced traditional methods with one of the many reasons being inferior surface quality. Surface texture plays a crucial role in the functionality of a component and can cause serious problems to the manufactured parts if left untreated. Therefore, it is necessary to fully understand the surface behavior concerning the factors affecting it to establish control over the surface quality.

The challenge with AM is that it generates surfaces that are different compared to conventional manufacturing techniques and varies with respect to different materials, geometries and process parameters. Therefore, AM surfaces often require novel characterization approaches to fully explain the manufacturing process. Most of the previously published work has been broadly based on two-dimensional parametric measurements. Some researchers have already addressed the AM surfaces with areal surface texture parameters but mostly used average parameters for characterization which is still distant from a full surface and functional interpretation. There has been a continual effort in improving the characterization of AM surfaces using different methods and one such effort is presented in this thesis.

The primary focus of this thesis is to get a better understanding of AM surfaces to facilitate process control and optimization. For this purpose, the surface texture of Fused Deposition Modeling (FDM) and Laser-based Powder Bed Fusion of Metals (PBF-LB/M) have been characterized using various tools such as Power Spectral Density (PSD), Scale-sensitive fractal analysis based on area-scale relations, feature-based characterization and quantitative characterization by both profile and areal surface texture parameters. A methodology was developed using a Linear multiple regression and a combination of the above-mentioned characterization techniques to identify the most significant parameters for discriminating different surfaces and also to understand the manufacturing process. The results suggest that the developed approaches can be used as a guideline for AM users who are looking to optimize the process for gaining better surface quality and component functionality, as it works effectively in finding the significant parameters representing the unique signatures of the manufacturing process. Future work involves improving the accuracy of the results by implementing improved statistical models and testing other characterization methods to enhance the quality and function of the parts produced by the AM process.

Keywords: Additive manufacturing, Fused deposition modeling, Laser-based Powder bed fusion, Power spectral density, Scale-sensitive fractal analysis, Feature-based characterization, Profile parameters, Areal surface texture parameters, Multiple regression, Stylus profilometer, Structured light projection, Confocal fusion.

ACKNOWLEDGEMENTS

I am grateful for the opportunity provided to me at Halmstad University and would like to take this moment to thank all the people who supported and helped me during my licentiate thesis.

Firstly, I would like to express my deepest gratitude to my supervisor Prof. Bengt-Göran Rosén for his continuous support, patience and encouragement throughout the development of this research work. His immense knowledge, experience and timely guidance allowed me to grow both personally and professionally.

My sincere thanks to my closest friend and colleagues, Vijeth Venkataram Reddy and Olena Flys for their guidance, cooperation and contribution. I am grateful to all my collaborators and co-authors for their inputs in my research.

I would like to extend my gratitude to all my colleagues at Halmstad University especially, Henrik Barth, Sabina Rebeggiani, Zlate Dimkovski and Pär-Johan Lööf for their endless help and valuable advice. Special mention to Johan Berglund from RISE for his guidance and support. Many thanks to Prof. Tom R. Thomas for his valuable comments on my thesis report.

Furthermore, I wish to thank Stefan Rosén from Toponova AB for his insightful comments and suggestions on surface metrology. Special thanks to Digital Surf for providing MountainsMap surface image analysis and metrology software.

Finally, I would like to thank all my friends for their support, especially Rakshith for his help with endless reasoning and guidance. I owe a debt of gratitude to my family, my mother, Meera and my father, Vedantha Krishna for their implacable love, support and unwavering belief in me. Without them, I would not be the person I am today. Above all, I would like to thank my wife, Vidya, for her unparalleled love, patience and constant support. She kept me going during my difficult times with never-ending motivation and kept me balanced during the past few months, this work would not have been possible without her.

LIST OF APPENDED PAPERS

Paper 1: Amogh V. Krishna, O. Flys, Vijeth V. Reddy, A. Leicht, L. Hammar and B.-G. Rosén. (2018) *Potential approach towards effective topography characterization of 316L stainless steel components produced by selective laser melting process.* In: European Society for Precision Engineering and Nanotechnology, Conference Proceedings - 18th International Conference and Exhibition, EUSPEN (pp. 259-260).

Paper 2: Amogh V. Krishna, O. Flys, Vijeth V. Reddy, J. Berglund and B.-G. Rosén. (2020) *Areal surface topography representation of as-built and post-processed samples produced by powder bed fusion using laser beam melting.* Journal of Surface Topography: Metrology and Properties, Volume 8, 024012.

Paper 3: Amogh V. Krishna, M. Faulcon, B. Timmers, Vijeth V. Reddy, H. Barth, G. Nilsson and B.-G. Rosén. (2020) *Influence of different post-processing methods on surface topography of fused deposition modelling samples*. Journal of Surface Topography: Metrology and Properties, Volume 8, 014001.

Paper 4: Vijeth V. Reddy, O. Flys, A. Chaparala, C. E. Berrimi, **Amogh V. Krishna** and B.-G. Rosén. (2018) *Study on surface texture of Fused Deposition Modeling.* Procedia Manufacturing, Volume 25, Pages 389-396, ISSN 2351-9789, 2018.

LIST OF ABBREVIATIONS AND SYMBOLS

AM	Additive Manufacturing
FDM	Fused Deposition Modeling
FFF	Fused Filament Fabrication
ASTM	American Society for Testing and Materials
ISO	International Organization of Standardization
SLA	Stereolithography
DLP	Digital Light Processing
CLIP	Continuous Light Interface Production
SGC	Solid Ground Curing
LPS	Liquid Phase Sintering
PBF-LB/P	Laser-Based Powder Bed Fusion of Polymers
PBF-LB/M	Laser-Based Powder Bed Fusion of Metals
PBF-EB/M	Electron Beam Powder Bed Fusion of Metals
EBM	Electron Beam Melting
EBAM	Electron Beam Additive Manufacturing
SLS	Selective Laser Sintering
DMLS	Direct Metal Laser Sintering
SLM	Selective Laser Melting
LOM	Laminated Object Manufacturing
UAM	Ultraviolet Additive Manufacturing
DED	Directed Energy Deposition
LENS	Laser Engineered Net Shaping
EBW	Electron Beam Welding
IIOT	Industrial Internet of Things
STL	Standard Triangle Language
ABS	Acrylonitrile Butadiene Styrene
CM	Confocal Microscope
FV	Focus Variation
FP	Fringe Projection
CCD	Charge-Coupled Device
CF	Confocal Fusion
λs	Low pass micro-roughness filter
λc	High pass filter
P	Primary
R	Roughness
W	Waviness
S	Surface
V	Volume
GPS	Geometrical Product Specifications
PSD	Power Spectral Density
ASME	American Society of Mechanical Engineers

A	Area
$h(x, y)$	Surface height map
$\mathscr{F}$	Fourier Transform
a	Lateral displacement in the spatial frequency domain in the x-direction
b	Lateral displacement in the spatial frequency domain in the y-direction
w	Width of the pixel
l	Length of the pixel
PSDF	Power Spectral Density Function
ANOVA	Analysis of Variance
R^2	Coefficient of determination
Lt	Layer thickness
α	Build inclination
Ra	Arithmetic mean deviation of roughness profile
Rp	Maximum peak height of roughness profile
Rz	Maximum height of roughness profile
Rdc	Roughness profile Section Height difference
Rv	Maximum valley depth of the roughness profile.
Rsm	Mean width of roughness profile elements
Rpc	Peak count on the roughness profile
Sa	Average Roughness
Sq	Root Mean Square Height
Smc	Inverse Material Ratio
Sal	Auto-Correlation Length
Str	Texture Aspect Ratio
Sdq	Root Mean Square Gradient
Sdr	Developed Interfacial Area Ratio
Vmc	Core Material Volume
Vvc	Core Void Volume
Vv	Void Volume
AVD	Acetone Vapour Deposition
LAF	Laser-Assisted Finishing
DOE	Design of Experiments
S/N	Signal to Noise ratio
LI	Low Infill
MI	Medium Infill
HI	High Infill
HQ	High Quality
MQ	Medium Quality

TABLE OF CONTENTS

1 INTRODUCTION

1.1 Background

Over the past decade, Additive Manufacturing (AM) has gained a lot of prominence for its ability to produce parts without geometrical limitations. Its potential to fabricate parts by deposition of materials layer by layer has re-defined manufacturing. A growing number of companies are leveraging AM to their advantage due to its several sustainability advantages. Customization, reduction of lead time, no assembly requirement, reduced wastages, lower energy intensity, reduced manufacturing costs, and reduced time-to-market are some of the benefits of this technique [1]. AM has been extensively used in automotive [2], aerospace [3], medical [4] and dental applications [5] for its ability to fabricate intricate lightweight designs and internal structures. The disruptive nature of AM has the potential to replace conventional manufacturing but mainly used as functional prototypes in many applications. This is mainly due to its inability to match the standards set by conventional manufacturing in terms of high-quality, reliability, performance and repeatability [6]. This has limited its widespread use in industries especially in critical applications, however, technological advancements in recent years have begun to slowly push AM from the prototyping stage to more advanced production of high-quality end products. Nonetheless, it is important to address the challenges of AM for encouraging its commercialization and for the realization of its economic benefits. One of the challenges of AM pertaining to surface quality is addressed in this thesis.

Typically, surface effects can cause up to 10% of failure rate in manufactured parts and with AM it can be even higher [7]. With an ever-increasing demand for manufactured goods, it is of great importance to have an efficient production system of high-quality products. Hence, it is necessary to fully comprehend the nature of AM surfaces to understand their manufacturing process in order to establish control over the quality and function of fabricated products. To achieve this, surfaces should be measured using appropriate metrology techniques and the captured surfaces must be characterized (requiring to describe typical characteristics or nature of surfaces) using various qualitative and quantitative methods.

The most widely adopted approach in extracting surface information is through a parametric description. AM surfaces consist of several features and to achieve a complete description of the surface, several parameters are often required. However, it must be realized that relatively large changes in some of these parameters may not affect the surface quality or functional performance of the parts [8]. In other words, every manufacturing processes generates unique surface features denoting the process signatures which largely affect the surface quality and function. Therefore, it is necessary to identify and analyze these significant features to understand the manufacturing process and to enable process optimization for improving the surface quality and function of the parts.

In the literature, the identification of significant surface features representing the manufacturing process signatures are often missed and a general description of the surface is provided through the use of average roughness parameters. This usually leads to an inadequate understanding of the manufacturing process and often hinders the correlation between the surface and its function. Hence, this thesis aims to address these research gaps by providing improved methods for the characterization of complex AM surfaces. This is accomplished by employing advanced characterization methods to get a better understanding of AM surfaces. It assists in analyzing the surface features at various scales or as a function of spatial frequency which are useful in identifying the most significant AM surface features. Furthermore, statistical approaches in combination with parametric characterization can be critical in

identifying the most important surface parameters which provide a quantitative description of significant surface features.

1.2 Aim of the thesis

The overall aim of this thesis is to establish the most effective approach towards topography characterization of Additive Manufactured surfaces to facilitate a better understanding of the manufacturing process for enabling process control and optimization. This is done by

a. Employing advanced surface topography characterization techniques to identify the unique surface features representing the manufacturing process signature.
b. Employing statistical methods to understand the relationship between surface texture and manufacturing process control variables.
c. Developing a methodology that uses both statistical and advanced methods to identify the significant parameters to discriminate between various surfaces and in turn, understand how the manufacturing process can assist in process optimization and control.

1.3 Research Questions

This thesis is based on the following three research questions.

1. How can the overall representation of AM surfaces be improved by using advanced surface topography characterization techniques?
2. How can statistical-based quantitative approaches and advanced methods towards surface characterization contribute to improving the understanding of AM and post-processes?
3. How can the developed research methodology interpret the scale-limited and multi-scale surfaces to enable process optimization?

1.4 Approach

The research approach adopted in this thesis is based on the control loop system first presented by Stout and Davis [8]. It comprises of three important facets namely manufacturing, characterization and function linked together in a loop as shown in figure 1. In this thesis, the primary focus is on the characterization, however, it can only be meaningful if it is associated with the manufacturing process and component function. Every manufacturing process can be interpreted by using topography characterization which in turn can be utilized to predict the functional behavior of the component and by knowing the function it is possible to refine and improve the efficiency of the manufacturing process.

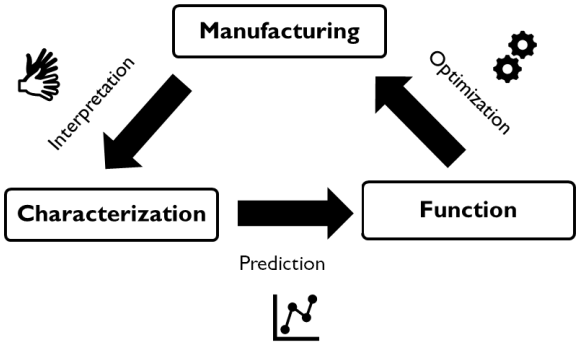

Figure 1. *Control loop depicting the interdependence of manufacturing, characterization and function.*

A detailed overview of the research approach based on the surface control loop is presented in figure 2. In this research, the surfaces of Fused Deposition Modeling (FDM) and Laser-Based Powder Bed Fusion of Metals (PBF-LB/M) produced by various AM process settings are subjected to various post-processing methods with variable settings to enhance the surface quality. Both the as-built and post-processed surfaces were captured using Stylus Profilometer, Structured light projection and Confocal Fusion optical microscopy. These captured surfaces were interpreted using advanced characterization techniques such as PSD, Scale-sensitive fractal analysis (Area-scale analysis), Feature-based characterization and statistical methods. In addition, a methodology was developed to identify the most critical parameters for characterizing the scale-limited and multi-scale surfaces to exploit the most essential factors affecting the functional behavior of the component. This established knowledge can be utilized in process optimization and control by adjusting the AM and post-process variables to match the functional and quality needs.

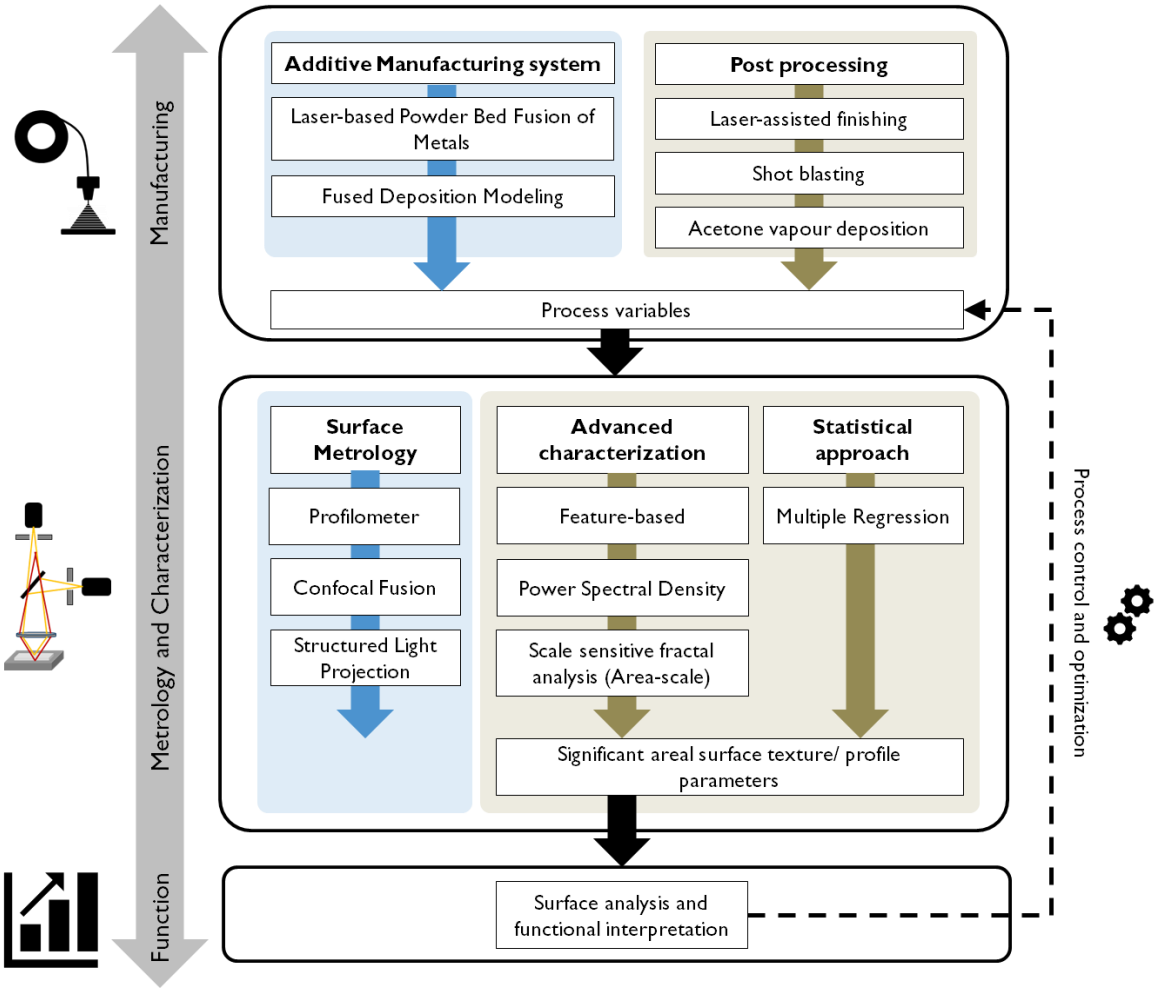

Figure 2. *Research approach as per the control loop for the development of functional surfaces of the AM process.*

1.5 Delimitations

- This research is confined to only FDM and PBF-LB/M techniques for surface analysis. Surface features differ significantly with change in AM technology and hence it will be necessary to study other techniques to generalize the findings obtained from this study.

- Surface metrology is confined to tactile and optical measurements which fail to capture the re-entrant features [9] of PBF based AM surfaces, because of this there may be some loss of surface information. It is necessary to explore the extent of the impact this lost surface information can cause.
- The research methodology is restricted to a linear statistical approach to study the influence of AM process variables on surface texture and to predict its functional behavior. The polynomial approach must be explored to determine if it can improve the prediction of surface quality and function.

1.6 Thesis structure

Chapter 1 provides a brief introduction highlighting the background, aim, research approach and limitations.

Chapter 2 presents an overview of Additive Manufacturing processes and post-processing methods and including associated surface conditions.

Chapter 3 describes the state of the art in surface metrology for AM processes.

Chapter 4 includes topography characterization techniques used for AM surfaces.

Chapter 5 outlines the research methodology.

Chapter 6 illustrates the results of the appended papers.

Chapter 7 reports conclusions and future work.

2 ADDITIVE MANUFACTURING SYSTEMS

2.1 Introduction

Additive Manufacturing (AM) popularly known as 3D printing is a fabrication technique involving the progressive deposition of material, layer by layer, leading to the creation of highly complex parts [1]. As per ISO/ASTM 52900:2015 standard terminology, Additive Manufacturing is described as the *"process of joining materials to make parts from 3D model data, usually layer upon layer, as opposed to subtractive manufacturing and formative manufacturing methodologies"* [10]. The unique technique of building parts layer by layer has provided industries with numerous advantages, which is why AM is considered as the emerging next-generation technology in part manufacture. Not until recently, did the patents on the original pre-existing printers expire which led to the rapid growth in the AM industry [1]. Today, there are several types of AM technologies which are broadly classified into seven categories.

- *Powder bed fusion* processes consist of a powder reservoir, platform, a thermal source and a powder recoating system. The re-coater spreads a layer of the material powder on the platform and the heat from the thermal source is utilized to melt and fuse the powders and then the platform is lowered to distribute a new layer of powder and the process repeats until the part is finished [11]. There are typically four types of powder fusion mechanisms, solid-state sintering, chemically induced sintering, Liquid-phase sintering (LPS) and full melting. The solid-state sintering involves fusion of the particles at elevated temperatures without melting. The chemically induced sintering process initiates the bonding process due to the thermally activated chemical reactions which create a by-product that fuses the powders together. LPS is a partial melting process where only some portion of the powders melt while others remain solid and the molten portions bind the other solid powders together. The full melting process completely melts the powder particles into a liquid which then undergoes a solidification process to build a part [1]. Furthermore, there are two types of thermal source, Laser-based methods use a laser beam in an inert atmosphere for producing metal, polymer, ceramics and composite materials. Electron beam uses electrons in a vacuum environment, as a thermal source to produce parts. Hence, it cannot be used to produce parts made of non-metallic materials such as polymers or ceramics. According to the ISO/ASTM 52911:2019 standard, the laser-based methods are termed as Laser-based Powder Bed Fusion of Polymers or Metals (PBF-LB/P or PBF-LB/M) and for an electron beam, it is called as Electron beam Powder Bed Fusion of Metals (PBF-EB/M). However, these technologies are known popularly by different names as given by AM technological providers. Selective Laser Sintering (SLS) process builds parts usually made of non-metallic materials [12]. Direct Metal Laser Sintering (DMLS) method works best with metal alloys and Selective Laser Melting (SLM) is used to produce parts made of metals [1][13]. Electron Beam Melting (EBM) or Electron Beam Additive Manufacturing (EBAM) works with metal and metal alloys and has higher productivity but limited materials compared to the laser-based methods [14].
- *Material extrusion* is by far the most popular AM technology on the market. According to the ISO/ASTM standards, extrusion refers to the process where the material is selectively discharged through a nozzle by application of pressure [10]. There are two types of extrusion-based AM processes, the most common one is the Fused Deposition Modeling (FDM) or Fused Filament Fabrication (FFF) method which uses temperature as the controlling mechanism for material flow [1][15][16][17]. The solid material is heated to its melting temperature, and the molten material is extruded layer by layer to build the part.

The other approach is quite the opposite, which uses a chemical reaction to cause the solidification process to build a component. For instance, Contour Crafting can be one such method where the "wet" quick setting concrete-like material is extruded layer by layer and it solidifies to build an object [18][19][20]. Another example is the 3D bio-printers which extrudes layer by layer of biomaterials to build 3D functional living tissues and organs [21][22][23].

- *Vat photopolymerization* is a process where liquid polymer or radiation-curable resin undergoes a chemical change to solidify upon the incidence of Ultra-violet rays or visible light portion of the electromagnetic spectrum [24]. The most common methods in this category as named by different AM technological providers are Stereolithography (SLA) [25] and Digital Light Processing (DLP) [26], it typically consists of a resin tank, build platform and light source. The main difference between these methods is the source of curing, the former uses Laser beam and the latter uses visible light from a projector. Continuous Light Interface Production (CLIP) [27] and Solid Ground Curing (SGC) [28] are recent advances in vat photopolymerization processes with the sole purpose to increase the fabrication rate.
- *Material jetting* process operates similarly to the 2D inkjet printers. In this technique, a printhead selectively sprays the photo-sensitive liquid material and UV light curing is performed after each layer of dispensed material droplets, the process repeats layer by layer thereby building an object [29].
- *Binder Jetting* comprises of several steps to build the part. Firstly, a recoating blade spreads a thin layer of material in powder form on the build platform. Then the print head deposits the binders (glue) selectively that bonds the powder particles together. After each layer, the build platform is lowered, and a new layer of powder is distributed, and the process repeats until the part is built. In the case of colored binder jetting, an additional step of coating the powder with colored ink is included, similar to the desktop 2D printers, to get vibrant colored end-products. Once the printing is complete, the part built is termed as a green part since it will usually be very brittle and porous and hence, it requires an additional curing step. Depending on the material, the curing step varies, typically for polymer products, the build part is left in the chamber after printing for binders to fully combine the powders. For metallic materials, the build part requires a sintering process or infiltration with low melting point metals to strengthen the part [1][30].
- *Sheet Lamination* is the process of combining sheets/layers of solid material together and using subtractive methods to shape it as per the required design. Laminated Object Manufacturing (LOM) and Ultraviolet Additive Manufacturing (UAM) are two types of process under this category. LAM is the process of laminating sheets of paper or plastic layer by layer and each layer of material is cut as per the shape of the cross-sectional layer of the designed CAD model and the cut layers are combined using adhesives to build an object [31]. UAM is a hybrid manufacturing process which uses both additive and subtractive methods to create a part. It combines sheets of metal foil using sonotrode and CNC milling is performed to shape it as per the designed object. Sonotrode is a tool that generates ultrasonic vibrations which are locally applied under pressure to metal foils to weld them together [32].
- *Directed Energy Deposition (DED)* is the process of building parts by melting material as it is being deposited [33]. The melting mechanism is similar to the conventional welding techniques, a thermal source focuses its energy into a narrow region where the material is supplied, simultaneously melting and depositing the material on a platform. There are wire-based and powder-based DED systems and the two popular methods are Laser Engineered

Net Shaping (LENS) and Electron Beam Welding (EBW) as the name suggests, a high powered laser beam or an the electron beam is used as a heating source to melt the material.

With the advent of Industry 4.0 and the Industrial Internet of Things (IIOT), the need for digital production is unprecedented. Although the technology push for AM has been exponential with the continuous development of new materials and processes, the procedure of part preparation for fabrication has been constant with all the AM technologies. An object to be printed is designed in the CAD modeling software and the 3D model is converted into STL (Standard Triangle Language) file format. The STL file is then sent to the 3D printing software where a slicing operation is performed, which converts the continuous geometry of the CAD model into a series of discrete layers. The printer then uses this information to fabricate the model layer by layer.

2.1.1 Additive Manufacturing as Sustainable Manufacturing

An increasing number of companies are embracing sustainable manufacturing due to its substantial environmental and financial benefits. With an ever-increasing demand for manufactured goods, the conservation of resources is very crucial in establishing long term benefits. Sustainable manufacturing is defined as the creation of goods through optimized processes that minimize the negative environmental impacts by conserving energy and natural resources [34]. Although sustainable manufacturing is a complex problem, the advent of Additive Manufacturing has made it easier for the industries to adopt sustainable business approaches. AM has several sustainability advantages such as limited usage of materials with minimum wastage during manufacturing; capable of producing intricate geometries and lightweight components and require comparatively less energy during manufacturing; and efficient inventory management since it is capable of producing parts on demand. This technological advantage aligns well with the goals of the United Nations sustainable development of responsible consumption and production [35], see figure 3. The overall articulation of *"AM as sustainable manufacturing of the future"* [36] is very promising, however, certain downsides of AM are limiting its widespread use in industries. The current scope of this thesis is to tackle one of the many challenges of AM by addressing the gaps concerning the surface quality. This thesis focuses on improving the understanding of the manufacturing process and enabling process optimization to enhance the surface quality and part function, thereby, helping the industries to implement AM into their supply chain.

Figure 3. *Sustainable development goals by the United Nations* [35].

In the following section, a detailed overview of AM technology utilized in this research is presented along with a brief explanation of the generated surfaces with their respective technology. The details of surface roughness mechanisms are provided to help readers visualize the common surface quality-related issues with AM.

2.2 Laser-based Powder Bed Fusion of Metals (PBF-LB/M)

This technique is also termed as Powder Bed Fusion – Laser Beam Melting. It consists of a laser source, laser beam focusing system, powder feed system and a control unit. The process takes place inside a closed chamber with an inert atmosphere mainly to avoid oxidation during the fabrication process. The metal powder is distributed over the build platform with the help of a powder re-coater. The laser beam from the sources is directed on to the powder bed in X and Y direction with the help of the high-frequency scanning mirror. The laser melts the powder layer as predefined by the sliced CAD file. The build plate is then lowered after the fabrication of one complete layer and then the powder is spread over this layer with the surrounding powder particles serving as support for subsequent layers. This continues until the part is completely built. Figure 4 displays the main components of PBF-LB/M system.

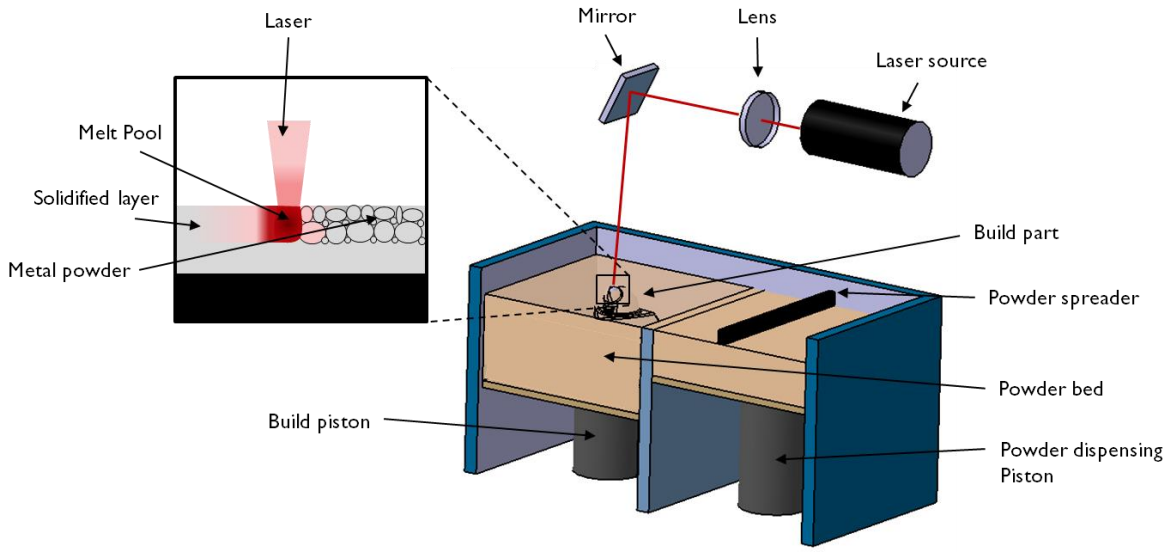

Figure 4. *Illustration of Laser-based powder bed fusion of Metals (PBF-LB/M) process.*

The input parameters influencing the part quality are powder particle size, material composition and properties, laser beam spot size, energy deposition, scan speed, atmosphere, material homogeneity, linear track separation, vertical step height, powder reuse, part geometry, scanning strategy and errors caused due to motion & energy deposition [37]. As mentioned by J S Taylor [38], characterizing the surface morphology helps to enhance manufacturing process control and attain stability in the essential physical processes. The input parameters induce the following physical processes such as conduction heat transfer, phase changes, radiation heat transfer, denuding effect, balling effect, spatter, melt pool size, pore formation, Rayleigh instability, Marangoni circulation, the evolution of grain structure, thermal expansion & shrinkage, spatial variation in temperature (heat sinks), 'stair-step effect', raster pattern and residual stress [37][38]. The surface morphology of PBF-LB/M is a result of the above-mentioned input parameters and corresponding physical processes.

Figure 5 shows the working principle of the PBF-LB/M technique with illustrations depicting the main contributing factor towards the development of surface roughness. In AM, the object is built in layers causing the slopes of the object to have a "stair-step" like structures

as shown in figure 5(a). The layer by layer manufacturing of PBF-LB/M causes the powder particles to adhere to the surface edges of each layer during the melting process. At 0° build inclination, most of the powder particles melt to form a solid layer. As the build angle/inclination increases the number of stair-steps increases leading to the decrease in the spacing of stair-steps (see figure 5(c)) and this, in turn, increases the adhesion of powder particles thus increasing the surface roughness. But beyond a certain build inclination, the surface roughness decreases due to the diminishing of the stair-step effect (see 90° surface). Surface roughness visualization for different build inclinations is provided in figure 5(c). This can be witnessed in figure 6, the 3D view of the surfaces generated at various build angles by the PBF-LB/M process. From the figure 6, it can be seen that lower build inclinations are dominated by a raster pattern (see 0° surface) and stair-steps effects (see 3° and 6° surface) and higher build angles beyond 15° are dominated by powder particles.

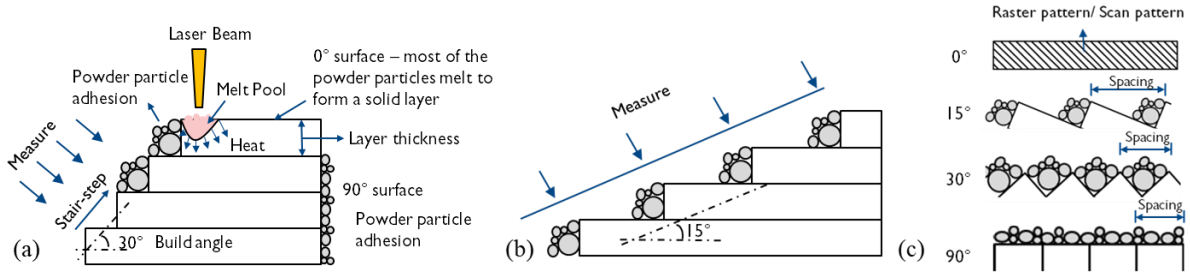

Figure 5. *Schematic representation of the PBF-LB/M process illustrating the mechanism of surface roughness development (a) at higher build inclination (b) lower build inclination and (c) visualization of surface roughness at various build inclinations.*

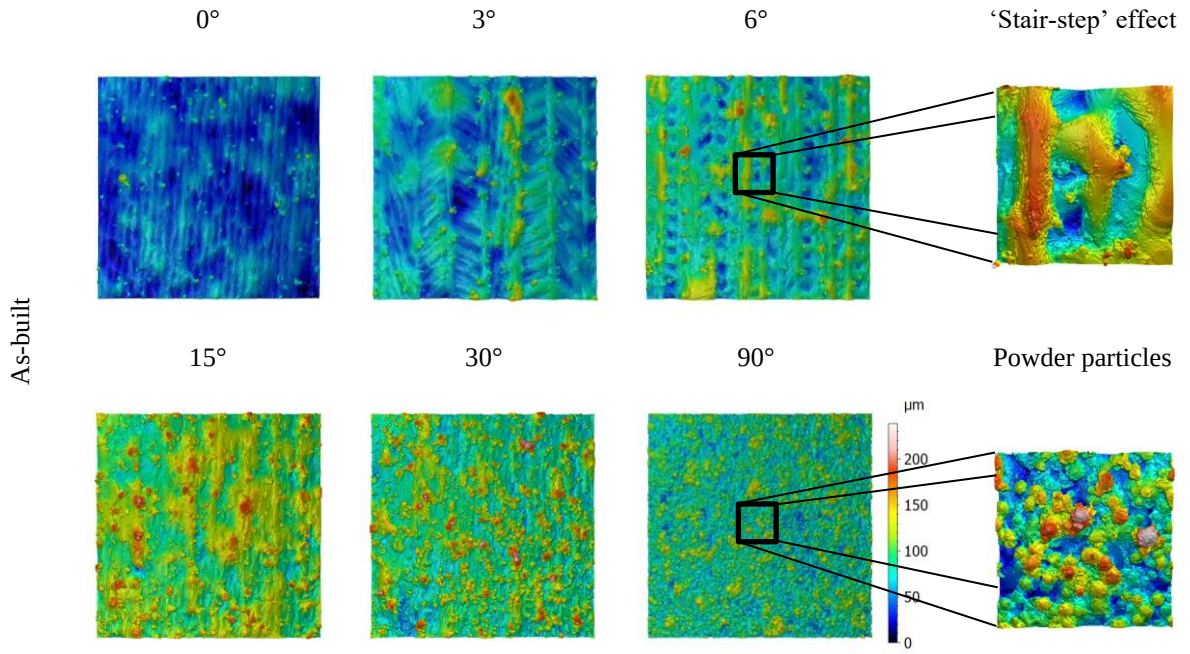

Figure 6. *3D topography view of as-built PBF-LB/M surfaces at various build inclinations. All surfaces have a measurement area of 2.5 mm×2.5 mm and the extracted surface has an area of 0.5 mm×0.5 mm.*

2.3 Fused Deposition Modeling

Fused Deposition Modeling (FDM) is a widely used extrusion-based AM process. Figure 7 shows an illustration of the FDM process. The material in the form of a wire from the filament spool is fed into the extruder by a step motor. The motor is fitted with a gear which pulls or pushes the material with the help of support bearing into the hotend. The material melts in the hotend and the molten material is extruded from the nozzle which is then deposited layer by layer on the platform to build an object. The whole extruder head is mounted on a fixture which provides the movement during printing [1].

In FDM, the part quality can be affected by various factors such as layer thickness, print temperature, print speed, infill settings, number of top layers and material properties. Apart from these, the geometry of the build part that is its build inclination (slopes) can have a large effect on surface quality. Much research has shown that the most dominating factor influencing the surface roughness is layer thickness and build inclination [39][40]. The development of surface roughness is similar to PBF-LB/M surfaces, FDM also has stair-step and raster pattern on its surface but is devoid of powder particles [41], see figure 8.

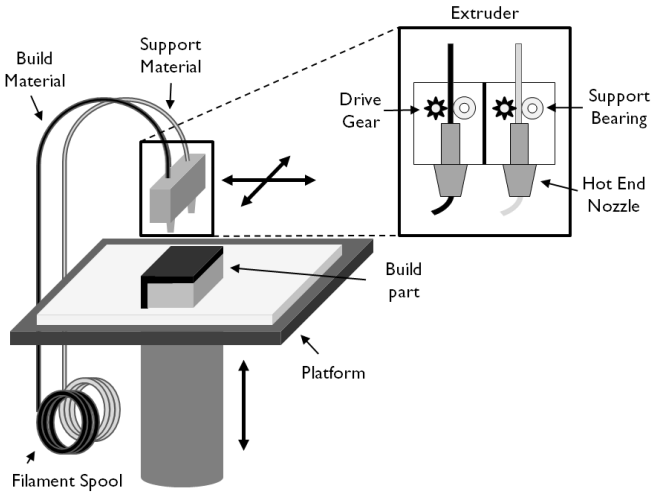

Figure 7. *Illustration of the FDM process*

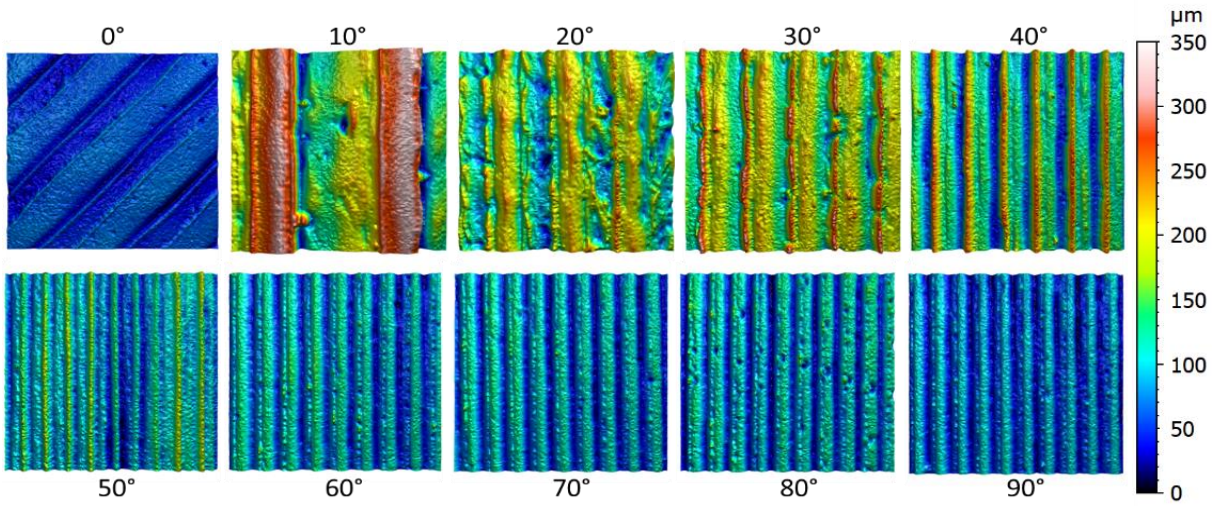

Figure 8*. The 3D view of surface topography of the as-built FDM sample with varying build inclinations to show the stair-step effect. All surfaces have a measurement area of 2.5 mm×2.5 mm.*

2.4 Post-processing

The principle of building components layer by layer makes it inevitable to eliminate features such as stair-step and raster patterns in AM surfaces. Although the effects of these features on surface roughness can be reduced by adjusting various print settings, the finish still cannot match the industrial standards in some cases. It is, therefore, necessary to use a subsequent post-processing step to finish the products. Although post-processing methods imparts high surface quality to the products, it increases the lead time and cost involved in manufacturing the end-product. However, this can be compensated by implementing Topology Optimization, i.e. performing design changes to reduce the material consumption and printing time without hindering the functionality of the component [42]. In this work, three post-processing methods are reviewed to find the best finishing process that can represent AM surfaces close to the conventional methods.

2.4.1 Shot-blasting

Shot blasting is a process of modifying the surface features by propelling a jet of abrasive particles at high pressure with the help of compressed air. The size and shape of the abrasive media, and the duration of blasting highly influence the surface roughness. Previous research has shown the effects of abrasive flow machining [43], abrasive jet deburring [44], and abrasive finishing of internal channels [45][46] on surface finish.

In this study, the surfaces generated by FDM and PBF-LB/M at various build inclinations were blasted to smoothen the surface and possibly produce surfaces close to the conventional manufacturing methods. Generally, sandblasting media is used for producing rough finish and glass beads for producing finer finish on the surfaces. This is because sand grains contain irregular shape and sharp features which when impacted on the surface creates an abrasive action damaging the surface, whereas, the glass beads appear comparatively smoother and rounder in shape which smoothens the sharp peaks and seals the pores on the surface upon impact [47]. Figure 9 represents the surfaces produced by shot blasting of FDM and PBF-LB/M surfaces, also, as-built surfaces produced by the respective AM techniques are provided for comparison. It is evident from figure 9 that the raster pattern as seen on the topography of the as-built surfaces in both FDM and PBF-LB/M techniques are removed due to the abrasive action of the shot-blasting process.

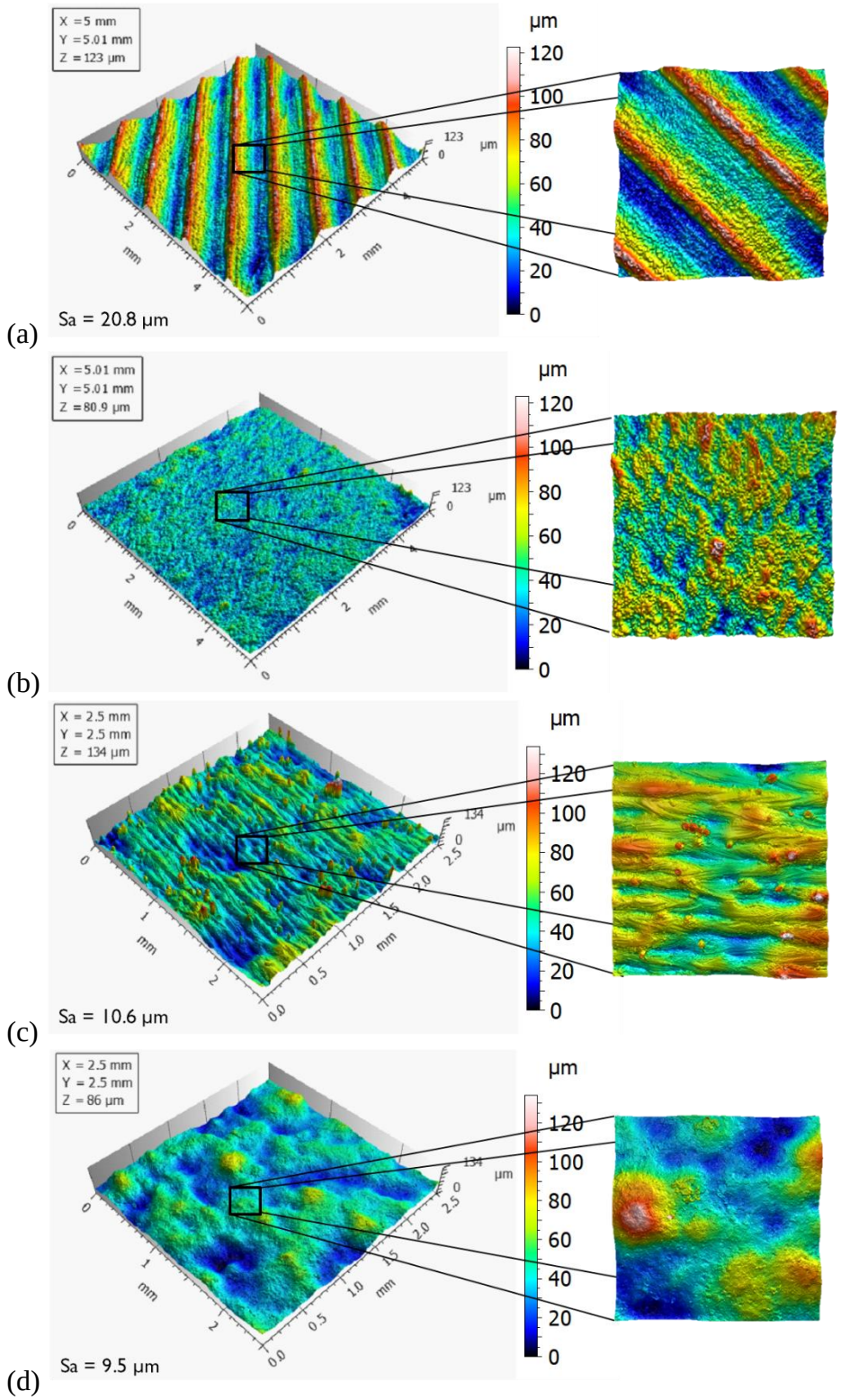

Figure 9*. The 3D view of surface topography at 0° build inclination (a) as-built FDM surface, (b) shot-blasted FDM surface; (c) as-built PBF-LB/M surface and (d) shot-blasted PBF-LB/M surface.*

2.4.2 Laser-assisted finishing

Laser-assisted finishing (LAF) is the process of smoothening the surface by focusing a high-powered laser beam on the sample which melts the top surface layer leaving behind a smoother texture. A Laser-assisted finishing process has been previously used for improving the surface conditions of FDM parts made of ABS (Acrylonitrile Butadiene Styrene) material [48]. Laser polishing [49] and Laser ablation [50] have been used to finish metal parts made from the SLM process. However, in this thesis, LAF was used for smoothening the FDM surfaces. The laser finishing process was carried out using a Trotec speedy 400 machine, which has a 120W high productivity CO_2 laser cutter with a working area of 1016 mm × 610 mm and a maximum height of 305 mm. A 4-inch lens with 7 mm diameter nozzle was utilized. Figure 10 illustrates the surface texture created by using this process for ABS material produced by the FDM process. The surface images showed in figure 10 were measured on the same sample produced by the FDM process before and after LAF process. The magnified surface texture of the laser-finished parts reveals the elimination of raster pattern and the anisotropy property of as-built surfaces.

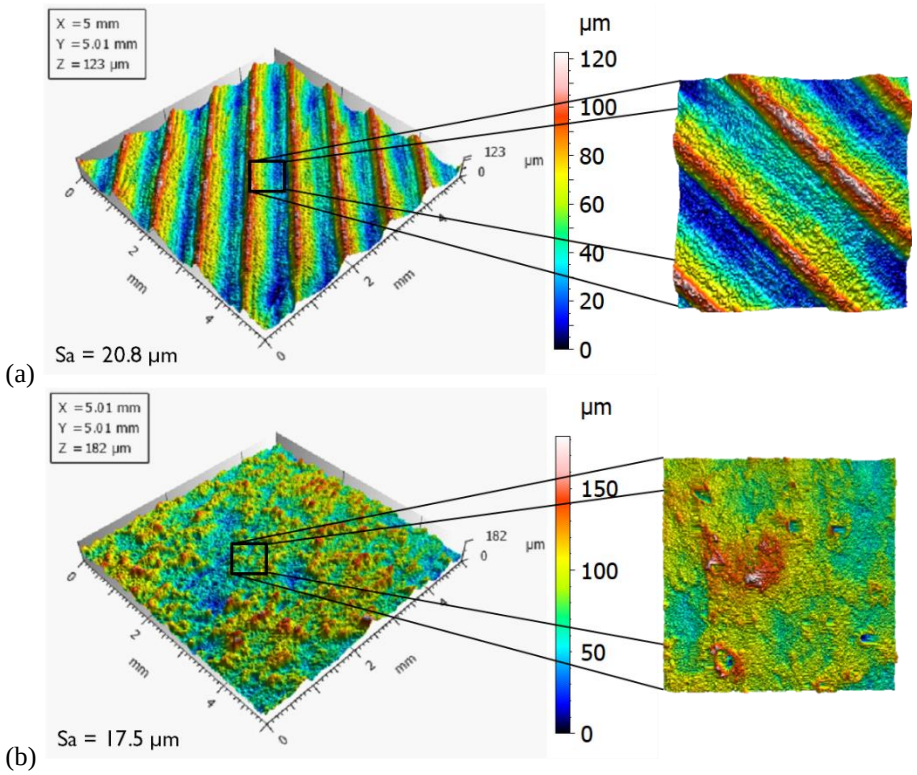

Figure 10. *The 3D view of surface topography of FDM surfaces at 0° build inclination (a) as-built and (b) laser finished surface.*

2.4.3 Acetone vapor finishing

In this study, the Acetone vapor smoothening was used to finish the thermoplastic polymer ABS material produced by the FDM process since ABS is highly corrosive to acetone. A simple set up was made for carrying out the acetone vapor finishing tests. An airtight box with its wall lined with a cloth containing some traces of acetone was utilized to finish the FDM part. The nano vapors of acetone get deposited on the sample and over time melt the plastic; therefore, it is necessary to remove the part in good time for best surface finish maintaining the dimensional quality. Figure 11 shows the surface topography of parts finished by this post-processing method. Research has shown that the factors influencing the surface finish using this method

are the acetone exposure time and the number of smoothening cycles. The former has a more significant effect than the latter on surface roughness [51].

The reaction of acetone with ABS material does not result in a chemical change in ABS thermoplastic, however, it can significantly change the geometrical shape of the ABS material. The layer by layer deposition of material during the FDM process creates the gap between the layers which is termed as ridges, as shown in figure 11a. Acetone reacts with ABS to form a molten thermoplastic slurry on the top layer. The semi-molten plastic then flows into the ridges creating a smooth and glossy finish (see figure 11b) [51]. Depending on the geometry of the part that has to be finished, the exposure time can vary.

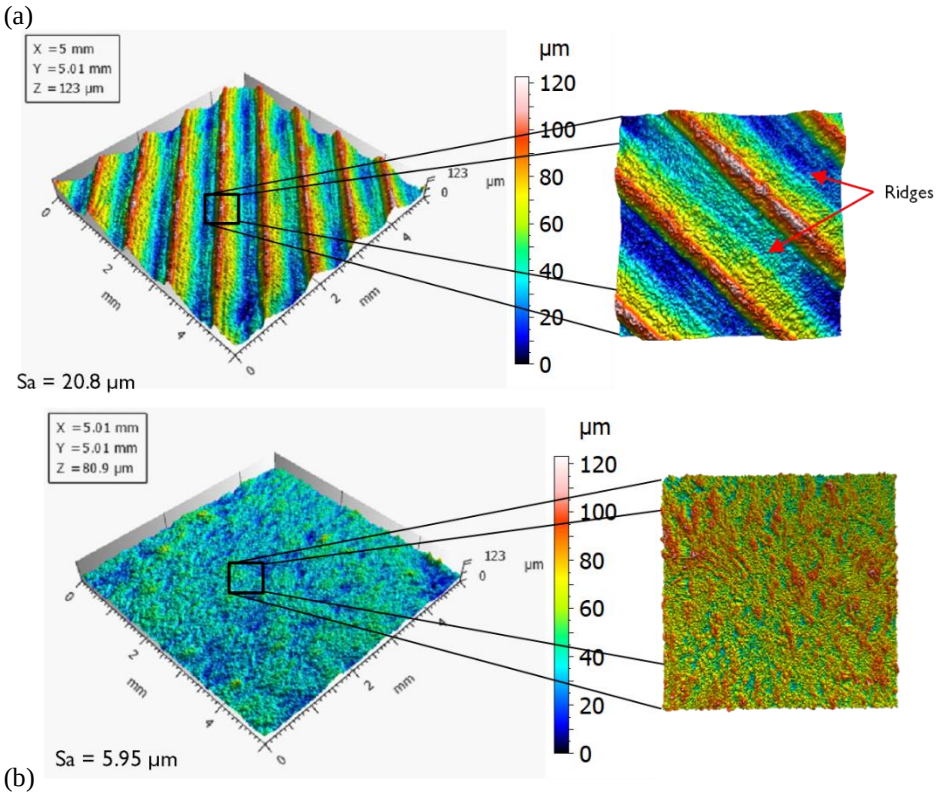

Figure 11. *The 3D view of surface topography of FDM surfaces at 0° build inclination (a) as-built and (b) Acetone-vapour finished surface.*

3 SURFACE METROLOGY

There is an increasing interest from manufacturing industries to gain control over the surface characteristics of their produced products since most of the component failures are surface-initiated [7]. Every manufacturing processes generates surfaces containing unique textures which sometimes can affect the ability of the product to perform its intended function [52]. It is therefore of high importance to study the surface texture for establishing control over the function and quality of the product. The studying of surfaces establishes an understanding of the effects of various manufacturing process variables on surface texture, which can then be utilized to engineer the surface to maximize the function and reduce failures. For this purpose, it is first necessary to capture the surface topography using an appropriate measurement technique to retrieve complete surface information. The established surface information can then be characterized both qualitatively and quantitatively to enable process optimization for achieving the best results.

Surface metrology is defined as the measurement of the complete geometric information about the surface shape and other irregularities caused by the manufacturing process [37]. In other words, it is defined as the measurement of the deviations of a workpiece from its intended shape and surface texture. The shape is referred to as form, which includes roundness, flatness, cylindricity and straightness [53]. Surface texture refers to the geometrical irregularities left behind by the manufacturing process [54]. With the advance of manufacturing technologies, surface metrology is increasingly facing challenges to characterize the surface features and the demand for new advanced analysis of surface features has increased to support innovation in the manufacturing industry. As a response to these demands, the International Organization of Standardization (ISO) published a standard, ISO 25178-6:2010 [55] which provides the classification of methods for measuring surface texture. As per the standard, there are three basic measurement techniques, line-profiling, Areal-topography and Areal integrating methods.

Line-profiling method is a technique of measuring the surface profile. It is achieved by measuring the geometrical deviations along the line scanned across the surface and can be mathematically represented as a height function with lateral displacement, $z(x)$ [56]. Examples of this techniques are contact stylus scanning [57], phase-shifting interferometry [58], circular interferometric profiler [59] (Measurement performed on circular profiles, mathematically represented as a height function with angular displacement, $z(\theta)$) and optical differential profiling [60].

Areal-topography method provides the surface information by generating the topographic image, mathematically given by $z(x,y)$ as a function of height with lateral displacements in x and y direction [55][56]. It can also be termed as topographic data obtained by combining a series of parallel profiles ($z(x)$ as a function of y). Examples of this method include confocal microscopy [61], coherence scanning interferometry [61], structured light projection, focus variation microscopy [62], digital holography microscopy, angle-resolved SEM, SEM stereoscopy [63], scanning tunneling microscopy, atomic force microscopy [64], optical differential profiler, point autofocus profiling.

Areal integrating methods provide numerical results dependent on area-integrated properties of surface topography [55]. Examples of this method are total integrated light scatter [65], angle-resolved light scatter [66], parallel-plate capacitance [67] and pneumatic flow measurement [68].

A brief explanation of some of the optical surface measurement instruments is provided elsewhere [7]. In the following section, an overview of different surface measurement techniques used in the study is presented.

3.1 Stylus Profilometer

The nominal characteristics of contact stylus instruments are defined in the ISO 25178-601 standard. It defines the stylus profilometer as a surface profile measurement system consisting of a probe with a contacting stylus whose motion is transformed into a signal as a function of position [69]. The stylus used in this instrument traverses a predefined distance over the surface and the vertical displacements caused by the irregularities on the surface are detected by the transducer which converts the signal into height data. The lateral movement of the worktable allows it to capture areal surface topography information by measuring a series of parallel profiles. The shape and radius of the curvature of the stylus tip along with sampling intervals determine the resolution of the profile. Typically, stylus tips are made of diamond material and have a radius of curvature ranging from 0.5 to 50 µm. Figure 12 shows a sketch of a stylus profilometer. The contact type measurement often causes deformations on the surface due to the contact of its hard stylus tip on the surface and repeated measurements over the same location are not recommended. Depending on the nature of surfaces under investigation, the deformation can be significant [70]. The measurement speed and load on the stylus tip may also contribute towards surface deformations and measurement errors. In this study, the stylus profilometer is utilized for measuring the surface profiles of Fused Deposition Modeling (FDM) samples. The highly anisotropic nature of FDM surfaces allows the captured individual profiles to be representative of the whole surface topography for analysis, as the profiles are measured perpendicular to the lay.

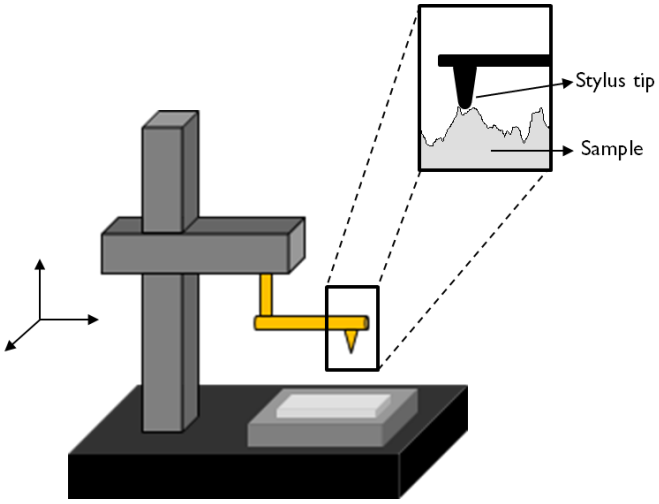

Figure 12. *Illustration of a Stylus Profilometer*

3.2 Structured light projection

Structured light projection, also known as Fringe projection (FP) is a "*surface topography measurement technique whereby a light image with a known structure or pattern is projected on a surface and the pattern of reflected light together with knowledge of the incident structured light can determine the surface topography*" [55]. This technique is termed as triangulation when the structured light is a single focused spot or fine line. Figure 13 displays the principle of this technique. It consists of a light source and camera to capture the images. A series of known patterns or fringes of light is projected onto the surface and a camera views the object under investigation from different perspectives. The surface features of the sample distort the projected pattern. The information obtained from the distorted light pattern along with the original incident light pattern can be used to reconstruct the surface topography data. Although this technique can be used to measure surfaces of a variety of materials, it struggles to capture

the data on reflective or transparent surfaces. In such cases, surface coating or using a replica can be recommended to capture the surface topography information.

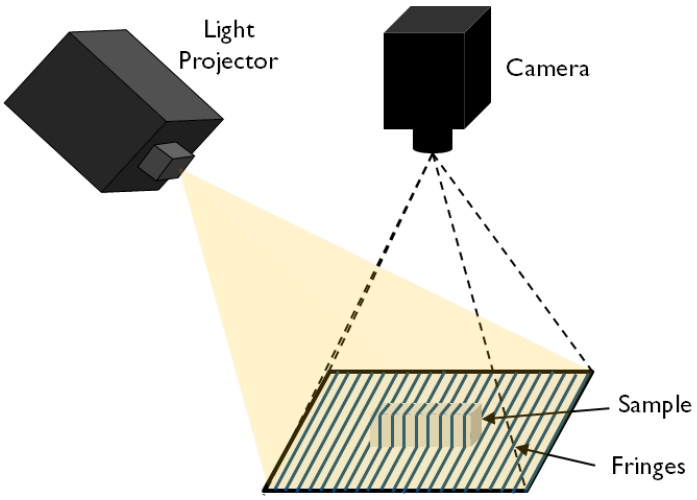

Figure 13. *Illustration of structured light projection technique*

3.3 Confocal microscopy

Confocal microscopy is one of the widely used optical techniques for measurement of surface topography. As the name suggests it has both the illumination and detector light paths on a common focal point [71]. The ISO 25178-602 provides the nominal characteristics of non-contact confocal chromatic probe instruments [72].

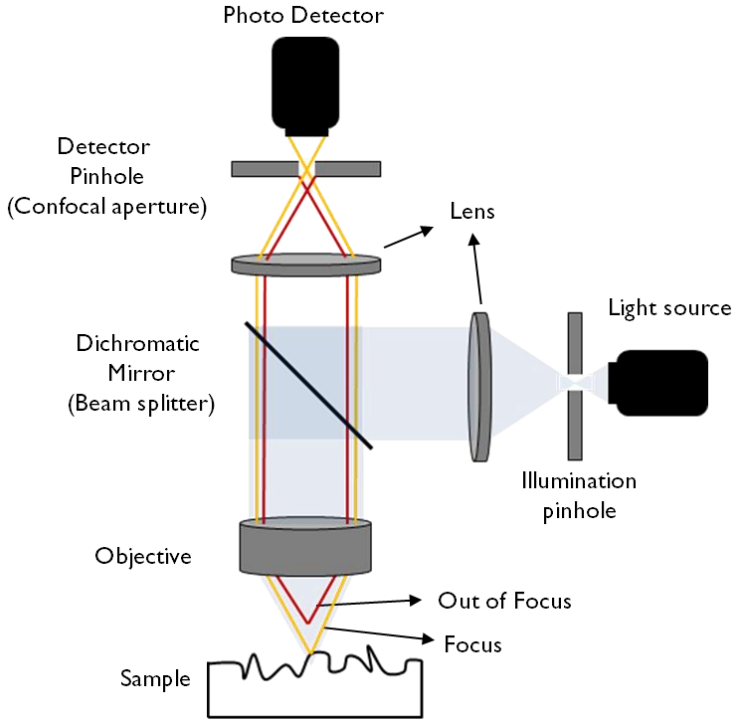

Figure 14. *Working principle of confocal microscopy*

The basic principle of confocal microscopy is presented in figure 14. It consists of two identically structured patterns in the form of pinholes, where one is placed near the light source and the other near the photo-detector. The light from the source passes through the pinhole

creating a structured illumination which is directed towards the dichromatic mirror onto the objective and the sample. The dichromatic mirror acts as a filter to remove certain wavelengths of light and allowing the remainder to pass through. Therefore, the reflected illumination from the sample passes through the dichromatic mirror and reaches the detector pinhole (confocal aperture) which permits only the focused light to fall onto the photo-detector and rejects the out of focus light. This makes it possible to produce optically sectioned images of the sample under investigation. A vertical scanning system is provided to move the objective to capture a series of optically sectioned images for analyzing different height regions of the sample. The images are captured by point by point illumination onto the surface. An optically sectioned image displays bright grey pixel levels for surface features that are in focus and dark for the rest of the regions that lie out of focus. This pixel intensity map from various optically sectioned images can then be used to reconstruct the 3D surface topography of the sample under inspection [7].

3.4 Focus Variation

Focus Variation (FV) microscopy is a surface topography measurement technique where the sharpness of the surface image is used to construct the surface height at each position along the surface [55]. Figure 15 illustrates the principle of this measurement technique.

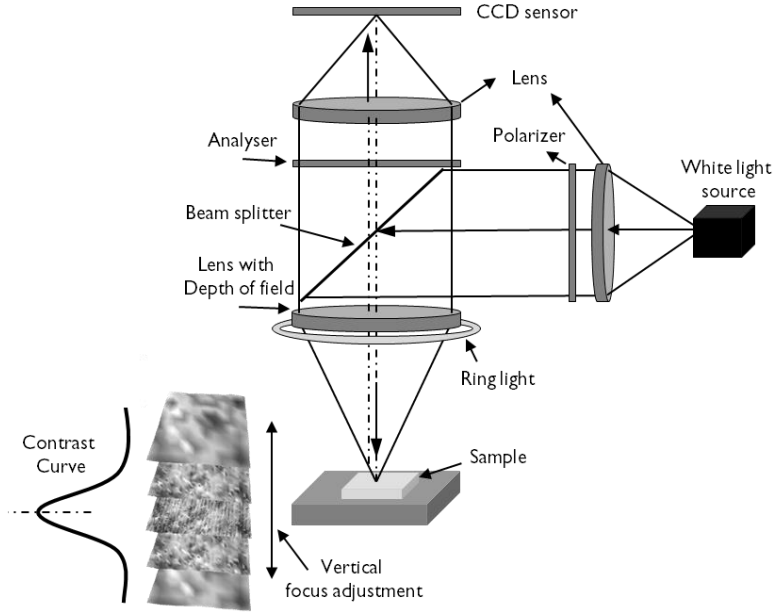

Figure 15. *Working principle of Focus variation microscopy*

A Focus variation instrument normally includes an optical system with limited depth of field for focus identification, light source, charge-coupled device (CCD) sensor and a drive mechanism [7]. Light from the source is transmitted through the beam splitter, semi-transparent mirror on to the objective and the sample. The irregularities on the surface scatter the light in different directions which are partially picked up by the objective and transmitted to the CCD sensor. The vertical movement of the sample relative to the objective varies the degree of focus of the sample surface and this change in focus causes the change in contrast in the CCD sensor. By analyzing the contrast on the CCD sensor, it is possible to reconstruct the height information of the surface under inspection. This principle of measurement enables FV to capture surfaces containing features with high slope angles. It is often used to measure the surface of Metal AM samples [73].

3.5 Confocal fusion

The measurement mode Confocal Fusion [74] is a combination of Imaging Confocal Microscopy and Focus Variation and is suitable to use with surfaces containing smooth parts as well as rougher parts with steep angles [74][75][76]. The surface topography of PBF-LB/M samples used in paper 2 was captured using this technology. The disadvantages of Focus variation and Confocal microscopy are avoided by this combined technique. As with all the individual "line of sight" instruments mentioned above (stylus profilometer, structured light projection, focus variation and confocal microscopy), confocal fusion technique also cannot capture the re-entrant features [9] present on the PBF-LB/M samples. Nonetheless, the captured surface was deemed enough for characterization.

4 TOPOGRAPHY CHARACTERIZATION METHODS

Surface measurement instruments provide the topography information that can be directly used for qualitative characterization and often a comprehensive quantitative method is required to fully understand the surface behavior. Before the surface analysis, it is important to process and refine the captured surface images so that they are suitable for characterization. Typically, the measured surfaces consist of geometrical information about surface shape and surface texture caused by its manufacturing process. Often, the surface shape is referred to as form and waviness; and surface texture is understood as roughness features of the surface topography. According to ISO 25178-2 [77], the primary surface is derived from the raw surface data after applying an S-filter which removes all the small-scale lateral components. S-F surface refers to the surface that is obtained from the primary surface after the application of F-operator to remove the form. S-L surface refers to the surface that is derived from S-F surface by removing the large-scale components using L-filter. The S-L surface is termed as roughness or surface texture and the residual surface after the application of L-filter on S-F surface is termed as waviness surface.

The difference between the form, waviness and roughness surface features is based on the surface wavelength [52]. The long-wavelength or low-frequency component on the surface topography is referred to as form. The occurrence of the form may be due to the geometrical shape of the sample being measured, it can be planar form due to tilt errors or rotary form when measured on cylindrical, cone or spherical samples. Waviness components on the surface topography usually have wavelength comparatively shorter than that of form. Waviness may occur due to disruptions such as vibrations, thermal effects during manufacturing or in some cases it may be due to the nature of the manufacturing process itself. For instance, during AM, the process of layer by layer manufacturing creates the effect of stair-steps on the surface which is considered as waviness. Once the form and waviness are removed the remaining geometrical irregularities on the surface topography are termed as roughness or surface texture. The separation of roughness and waviness is arbitrary, based on the nature of manufacturing processes or from the intended function of the sample, so an appropriate filter must be applied [52].

All the image processing operations on the captured surface topography were performed using MountainsMap, a 3D imaging and analysis software tool from Digital Surf [78]. The raw surface measurement data was pre-processed to remove the aberrations or any abnormality before the analysis. The form was removed by various algorithms such as levelling line by line, by least-squares method, levelling by partition and using a polynomial approximation to remove any shape from the surface topography. Based on the nature of the surface under inspection, suitable form removal operation can be employed. Once the form is removed, the waviness and measurement noise can be filtered from the roughness profile or surface by employing various filters such as Gaussian filter, spline filter, morphological filter, motif method, wavelet transform and spatial filters [79]. A brief explanation can be found in [80]. The quality of separation of roughness and waviness features of the surface depends on the type of filter and the nesting index value. The nesting index is the separation criteria based on wavelength threshold of the surface [79]. In addition, the surface captured by the optical microscope may not always have all the measured data points within its field of view due to the reflectivity or transparency issues of the sample. This can be handled in the software, where the non-measured points can be filled in by calculating the neighboring data points or filling it by a certain constant value. Once the surfaces are processed as required, it can then be subjected to various characterization techniques.

4.1 Parametric characterization

4.1.1 Profile roughness parameters

Profile roughness parameters have been a widely accepted method for characterization. The captured raw profile is processed to remove the micro-roughness and the resulting profile is termed as the Primary profile. The ISO 4288 [81] defines the selection of low pass micro-roughness filter λs which removes high frequency - short wavelength profile features as per the cut-off. Application of high-pass Gaussian filters λc as per ISO 16610-21 [82] to the primary profile results in two profiles namely roughness and waviness profiles. The parameters are calculated on each of these profiles have a prefix as P, R and W indicating primary, roughness and waviness profiles respectively. The parameter definitions and explanation of parameter groups can be found in [83][84]. Table 1 shows the parameters that are calculated on the roughness profile as per ISO 4287 [85].

Table 1. *Classification of profile roughness parameters as per ISO 4287*

Symbol	Unit	Parameters description	Parameter Group
Rp	µm	Maximum peak height of the roughness profile.	Amplitude Parameters
Rv	µm	Maximum valley depth of the roughness profile.	
Rz	µm	Maximum Height of roughness profile.	
Rc	µm	Mean height of the roughness profile elements.	
Rt	µm	Total height of roughness profile.	
Ra	µm	Arithmetic mean deviation of the roughness profile.	
Rq	µm	Root-mean-square (RMS) deviation of the roughness profile.	
Rsk	-	Skewness of the roughness profile.	
Rku	-	Kurtosis of the roughness profile.	
Rp1max	µm	Maximum local profile peak height	
Rv1max	µm	Maximum local profile valley depth	
Rz1max	µm	Maximum local height of the profile	
RSm	mm	Mean width of the roughness profile elements.	Spacing parameters
Rdq	°	Root-mean-square slope of the roughness profile.	
Rmr (c)	%	Relative Material Ratio of the roughness profile.	Material ratio parameters
Rdc (p, q)	µm	Roughness profile Section Height difference	
Rmr (Rz/4)	%	Automatic relative material ratio of the roughness profile.	
RPc	1/cm	Peak count on the roughness profile.	Peak parameter

4.1.2 Areal surface texture parameters

Topography characterizations are based on the areal surface parameters according to geometrical product specifications (GPS) – ISO 25178-2:2012, which specifies terms, definitions, and parameters for the determination of surface texture by areal methods [77]. Most of these parameters are the direct counterpart of profile parameters with additional parameter groups describing the areal surface topography. It is usually denoted by symbol S or V

indicating surface and volume respectively. Unlike profile parameters, the prefixes of areal surface parameters do not indicate the nature of the surface, discrimination between waviness and roughness surfaces. It is, therefore, necessary to associate the surface parameter values with the filtering conditions. The ISO 16610 presents various areal filtering methods to process the surface for analysis.

Table 2. *Classification of areal surface texture parameters as per ISO 25178-2*

Symbol	Unit	Description	Parameter Group
Sq	µm	Root-mean-square height	Height
Ssk	-	Skewness	
Sku	-	Kurtosis	
Sp	µm	Maximum peak height	
Sv	µm	Maximum pit height	
Sz	µm	Maximum height	
Sa	µm	Arithmetic mean height	
Smr (c)	%	Areal material ratio	Functional (Height)
Smc (p)	µm	Inverse areal material ratio	
Sxp (p, q)	µm	Extreme Peak Height	
Sal (s)	µm	Auto-correlation length	Spatial
Str (s)	-	Texture-aspect ratio	
Std	°	Texture direction	
Sdq	-	Root-mean-square-gradient	Hybrid
Sdr	%	Developed interfacial area ratio	
Vm (p)	$\mu m^3 / \mu m^2$	Material volume	Functional (Volume)
Vv (p)	$\mu m^3 / \mu m^2$	Void volume	
Vmp (p)	$\mu m^3 / \mu m^2$	Peak material volume	
Vmc (p, q)	$\mu m^3 / \mu m^2$	Core material volume	
Vvc (p, q)	$\mu m^3 / \mu m^2$	Core void volume	
Vvv (p)	$\mu m^3 / \mu m^2$	Pit void volume	
Spd	$1 / \mu m^2$	Density of peaks	Feature
Spc	1 / µm	Arithmetic mean peak curvature	
S10z	µm	Ten-point height	
S5p	µm	Five-point peak height	
S5v	µm	Five-point pit height	
Sda	μm^2	Mean dale area	
Sha	μm^2	Mean hill area	
Sdv	μm^3	Mean dale volume	
Shv	μm^3	Mean hill volume	
Sk	µm	Core roughness depth	Functional (Stratified)
Spk	µm	Reduced summit height	
Svk	µm	Reduced valley depth	
Smr1	%	Upper bearing area	
Smr2	%	Lower bearing area	
Svq	-	Valley root-mean-square roughness	
Spq	-	Plateau root-mean-square roughness	
Smq	-	Material ratio at plateau-to-valley transition	

Table 2 shows the list of areal surface texture parameters which are broadly classified into 7 groups.

Height parameters are groups of parameters that describe the surface features in the z-direction perpendicular to the surface. There are several parameters within this group each describing different aspects of the surface height. Average roughness parameters provide the overall measure of surface texture and can be used to differentiate various manufactured surfaces; skewness and kurtosis provide the shape of the surface topography height distribution and sharpness of the surface features respectively. Other parameters explain different amplitude features such as peaks and valleys.[56]

Spatial parameters are used to provide the characteristics of surface texture using spectral analysis. These parameters provide lateral information on the surface under inspection. Auto-correlation length (Sal) provides the measure of length along the surface such that the new location has a minimum correlation to the original location. Texture aspect ratio (Str) provides the measure of isotropy or directionality of the surface and Standard texture direction (Std) can be used to find the orientation of the dominant texture on the surface topography.[56]

Hybrid parameters are used to characterize the features that depend on both the amplitude and the spacing. These parameters provide information on surface intricacy, which can be used to discriminate between surfaces having similar average roughness.

Feature parameters are used to quantify the specific characteristics of the surface topography. The significant features on the surface topography are segmented and identified by a discrimination method known as pruning [56].

Functional parameters are a set of parameters used to characterize the functional aspects of the surface topography such as lubrication, wear and grinding. There are two classes of functional parameters, *height* and *volume* parameters usually provide the amount of material or void between predefined thresholds. They are calculated from the Abbott-Firestone curve (material ratio curve) which is the graphical representation of the cumulative distribution of surface amplitudes as a percentage of material [84][86]. *Stratified* parameters are used to describe the surfaces containing two or more types of textures imposed at different depths usually formed due to processing with different manufacturing methods. The surface may have several functional behaviors which can be quantified using parameters of this group [87].

4.2 Advanced characterization

4.2.1 Power spectral density

The power spectral density (PSD) is the representation of the surface texture amplitude as a function of the spatial frequency. According to ASME B46.1-2002, 2D PSD is defined as the square of the amplitude of the Fourier transform of the surface normalized by the area size of a pixel [88]. The areal surface texture can be represented as an integration of a series of roughness profiles and each roughness profile resembles a mixture of sine waveforms with varying frequencies. The Fourier transform decomposes these signals into individual frequencies. The Fourier transform of surface height map *h (x, y)* is given by

$$\mathcal{F}\{f(a,b)\} = \int_{-w/2}^{w/2} \int_{-l/2}^{l/2} h(x,y) e^{-2\pi i(ax+by)}\, dx\, dy \qquad (1)$$

Where, *h(x,y)* is the surface height data with lateral displacements or surface positions in *x* and *y* directions; *a* and *b* are the lateral displacements in the spatial frequency domain; *w* and *l* are the lateral resolutions representing the width and length of the pixel;

As per the definition, PSD is given by,

$$PSD\ (a,b) = \frac{1}{A}|\mathcal{F}\{f(a,b)\}|^2 \tag{2}$$

$$PSD\ (a,b) = \frac{1}{wl}\left|\int_{-w/2}^{w/2}\int_{-l/2}^{l/2} h(x,y)e^{-2\pi i(ax+by)}\,dx\,dy\right|^2 \tag{3}$$

Where A is the area of the pixel of the surface measured. Usually, the lateral resolution of the optical microscopes is same and hence $w = l$ *and* $A = l^2$. Therefore,

$$PSD\ (a,b) = \frac{1}{l^2}\left|\iint_{-l/2}^{l/2} h(x,y)e^{-2\pi i(ax+by)}\,dx\,dy\right|^2 \tag{4}$$

A detailed mathematical representation of PSD is provided in [89][90][91]. The PSD function has been widely used for characterizing optical surfaces [90] and often for polished surfaces. This spectral analysis tool is very useful as it provides an intuitive overview of the surface features at various wavelengths. In this thesis, the calculations of PSD are carried out using an Image Metrology's Scanning Probe Image Processor software. It offers a platform to compute the PSD for a given surface, however, it is crucial to understand the correctness of the results obtained as different calculations (windowing and smoothing function, selection of PSD algorithm based on the nature of surface) can lead to different results [80].

4.2.2 Scale-sensitive fractal analysis

Laser-Based Powder Bed Fusion of Metals (PBF-LB/M) surface consists of many significant features at various scales of observation and are often collectively represented at a single scale using the standard roughness parameters. This occasionally leads to inaccuracies in the results, particularly when identifying the differences in surfaces or correlation between the parameters and its functional behavior [92]. For instance, surface parameters may not be very effective in finding the surface defects caused by vibrations or other environmental conditions, which can easily be detected by analysis of surface features at various scales of observation. It is, therefore, important to identify the most important scale for characterization. For this purpose, the surface measured from the optical microscope is subjected to scale-sensitive fractal analysis.

Scale-sensitive fractal analysis [88][93][94][95] is a multi-scale approach which includes Area-scale and Length-scale analysis based on fractal methods. In this thesis, importance is given to *area-scale analysis* which calculates the area of the surface as a function of scale [93]. In this method, the relative area and complexity of the surface can be calculated. This is done by employing a virtual tiling algorithm in which the surface topography measured is covered with triangular tiles, as shown in figure 16. Each tile has the same area and represents a scale of measurement. The relative area at a particular scale is estimated by taking the ratio of calculated area to the nominal area at that scale. The calculated area is the product of the number of triangular tiles used to cover the surface and the scale or area of a single tile. The nominal area is the area projected by the triangles on the datum plane. Complexity is the measure of the slope of the relative area plot at each scale multiplied by orders of magnitude [92].

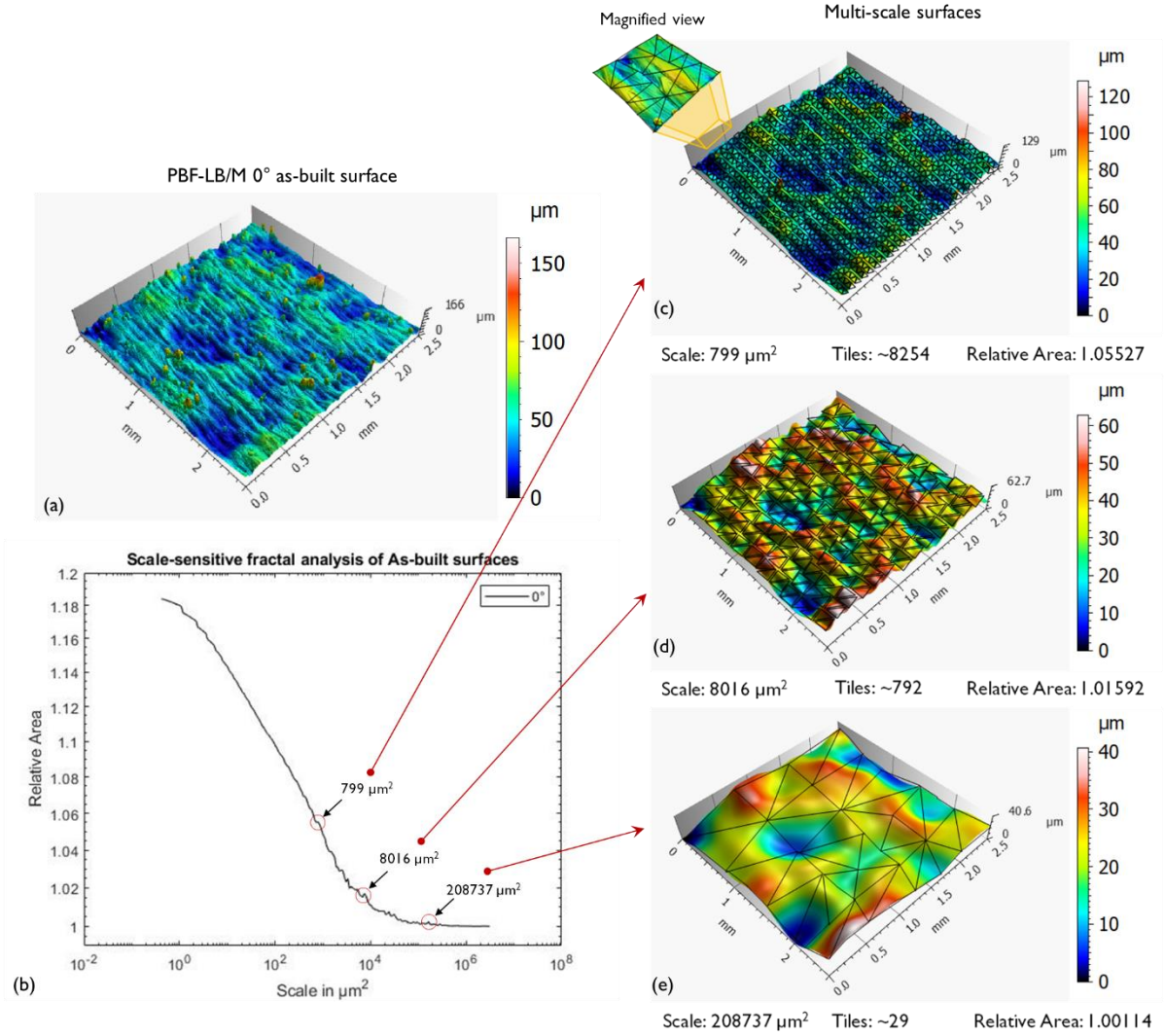

Figure 16. *Area-scale plots showing an example of tiling algorithm performed on an as-built PBF-LB/M surfaces at 0° build inclination. (a) Original surface (b) Relative area curve as a function of scale; (c-e) Surface topography representation at three different scales.*

4.2.3 Feature-based characterization

Several strategies have been discussed for the characterization of AM topographic features [96][97] and in this study, a discussion on an alternative characterization strategy to define the PBF-LB/M surface features is presented. Feature-based characterization refers to the process of separating the significant surface features and individually characterizing such features to fully understand the surface behavior concerning the factors affecting it. This is achieved in two steps.

Firstly, a robust Gaussian filter (ISO 16610-71) is employed to separate the waviness and roughness surfaces. The selection of the nesting index for filtering depends on the nature of the surface under investigation. The separated waviness surface would include the staircase effect [98] caused by the build orientation and also the form due to thermal conditions (shrinkages or swelling effects) during the build [98]. The roughness surface obtained includes powder particles and additional footprints of the process.

Secondly, a binary thresholding method is employed which helps in isolating the powder particles from the roughness surface by moving a plane from the highest point on the surface to the value of material ratio corresponding to the parameter Spk (Reduced summit height) of

the surface, provided the surface waviness is removed by the Robust Gaussian filtering. Powder particles thus obtained could contain unmelted or partially melted particles, balling effect and agglomeration of powder particles [37]. For ease of analysis, the characterization of powder particles is based on the collective volume of all the particles above the threshold. Once the powder particles are removed from the roughness surface, the residual surface contains the additional footprints of the PBF-LB/M process. Both the waviness and the residual surface can be subjected to characterization by areal surface texture parameters (ISO 25178-2). An example of the methodology in use is provided in figure 22 in the section 6.1.

5 RESEARCH METHODOLOGY

A wide range of parameters is required for describing the entire geometrical information of the surface relating to its shape of valleys and peaks, curvatures, texture, waviness and form. It is important to realize that all of these parameters may not necessarily explain the functional behavior of the component. It is, therefore, necessary to extract the most critical parameters that define the surface relating to its functional behavior. In the following section, a methodology is presented to identify the significant surface/profile parameters for both scale-limited and multi-scale surfaces which provide an improved understanding of the manufacturing process to predict the functional performance of the component.

5.1 Identification of Significant parameters

5.1.1 For scale-limited surfaces using linear multiple regression

Multiple linear regression is applied to scale-limited surfaces to identify the significant parameters. As the name suggests, scale-limited surfaces refer to the surfaces that are captured at a particular scale. It is usually referred to as S-F surface or S-L surface [77]. S-F surface is the surface that is derived from the raw surface after applying S-filter to remove small lateral wavelength components and F-operator to remove the form effects. S-L surface refers to the surface obtained after application of L-filter to S-F surface to remove large wavelength components. To simplify, the scale-limited surface is referred to as waviness or roughness surface captured at a particular scale of observation.

Regression analysis is the most commonly used statistical tool for modeling the relationship between the dependent variables and independent variables [99][100]. In this study, the dependent variables are surface/profile parameters and independent variables refer to AM process settings such as layer thickness, print temperature/speed etc., post-process settings, and sample geometry. Simple linear regression uses a linear model to predict the outcome of dependent variables with one independent variable, and for more independent variables it is termed as multiple linear regression. Furthermore, Analysis of variance (ANOVA) is a special case of regression analysis which explains the difference between means of two or more groups.

Figure 17 shows the methodology to identify significant parameters along with recognition of crucial process variables affecting it. Surfaces produced from various manufacturing process variables were captured and subjected to parametric characterization. The regression analysis was performed from the observed data of both independent and dependent variables. The interpretation of regression output is important to identify the relevant parameter and it is done by mainly observing the following factors.

Coefficient of determination, R^2 explains how the differences in one variable are explained by the difference in the second variable. Concerning the surface analysis, R^2 provides the proportion of variance in parameter readings that is predictable from the independent variables. The R^2 assumes that every independent variable in the model explains the variation in the dependent variable. This may not necessarily be true as some variables may not help in predicting the dependent variable. In such cases, adjusted R^2 can be useful, which identifies only those independent variables that explain the variability of dependent variables. Usually, adjusted R^2 is used when comparing the models with several independent variables. It can be understood that if the deviation between the R^2 and adjusted R^2 is high, then one or more independent variables may be ineffective in explaining the variations in surface parameter readings. In such cases, the model may be tweaked to improve its accuracy by excluding such independent variables or to include interaction effects of the independent variables. The adjusted R^2 also assists in evaluating the model fit. Once the regression analysis is established,

a threshold is set at a certain value of the R^2 or adjusted R^2 to filter out the parameters with the highest correlation.

Significance F provides an understanding of the reliability of the regression data. The probability of the measurements with respect to the process variables is reliable if the p-value associated with F-test is less than 0.05. It can also be understood as to what extent are independent variables reliable in predicting the variations in the surface parameter readings. The parameters that pass through the above-mentioned conditions are termed as significant. Once all the significant parameters are established, the next step is to identify which independent variable has a significant effect on surface parameters.

P-value- helps in determining the influence of process variables on surface or profile parameters. It is usually used to test the null hypothesis to quantify the statistical significance of measured data in the chosen t-statistic. The null hypothesis is a general statement claiming that the relationship between two measured variables (in this case, the two variables are surface parameters and process variables) is non-existent. If the p-value is less than 0.05 then it rejects the null hypothesis by stating that there is a valid relationship between the measured surface parameters and process variables.

Furthermore, *regression coefficients* obtained from the analysis describes the relationship between the dependent and independent variables. It is possible to model and predict the values of surface parameters for various values of chosen dependent variables. The positive value of regression coefficients indicates that the increase in independent variable results in the increase of the dependent variable. The negative value indicates that the decrease in the value of independent variables leads to a decrease in the value of dependent variables.

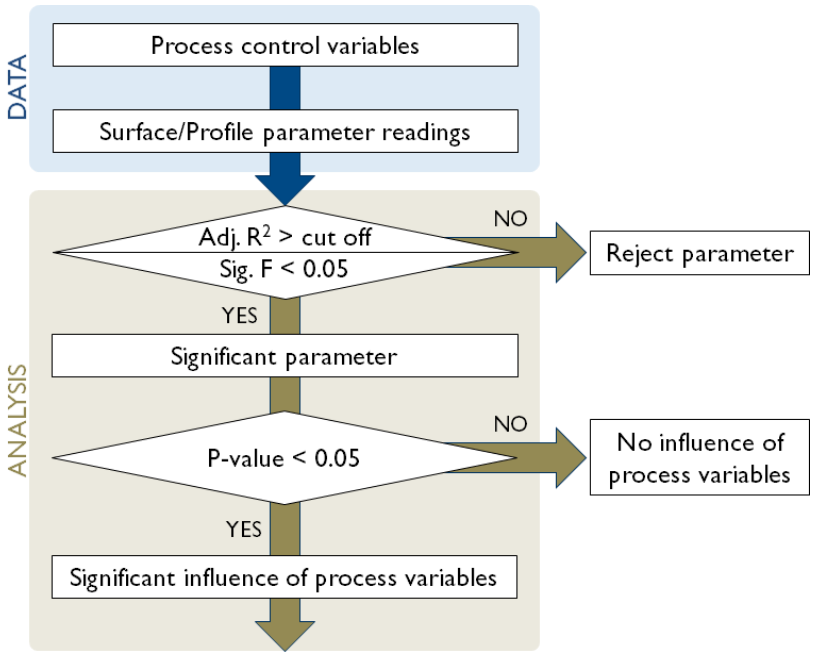

Figure 17. *Selection of significant parameter and influence of process variables using regression analysis.*

5.1.2 For Multi-scale surfaces using area-scale analysis

The multi-scale analysis presents the captured surface topography information from various scales of observations. Multiple surfaces can be obtained by filtering the surface at various nesting index wavelengths. This provides an opportunity to identify the most critical surface regions affecting the function and the developed methodology (see figure 18) helps in

identifying the significant parameters corresponding to these regions. The methodology works efficiently in discriminating the surfaces with limited independent variables influencing the surface parameters. For instance, the scenario presented in paper 2 identifies as-built and shot-blasted surface conditions along with variation in build inclination. In this context, two independent variables (process and build inclination) are influencing the change in response or dependent variable (surface parameters) and this comparison is made at various scales. This provides a deeper understanding of the manufacturing process which can facilitate process optimization to improve the surface function.

Area-scale analysis is performed for each of the captured surfaces and the complexity plots are obtained for both as-built and shot-blasted conditions. The complexity plots provide the rate of change in the surface intricacy from scale to scale. The complexity plots of both as-built and shot blasted processes are divided to explain the true difference between the two processes. The resulting plot is termed as 'Transfer function' and it is used to identify the important scale range where the difference between the two processes is maximum (see figure 25, in paper 2). The identified scale of interest is then extracted from the original surface by employing bandpass filtering using the robust Gaussian filter. The obtained filtered surfaces are subjected to parametric characterization to explain the differences between the two processes. Furthermore, the most significant parameters are identified within the selected scale regions. This is done by calculating the coefficient of determination (R^2) between complexity values and areal surface texture parameters at each scale [101]. The R^2 values are plotted for each scale and the parameters with the highest R^2 within the identified scale of interest are considered as significant parameters (see figure 26 in paper 2).

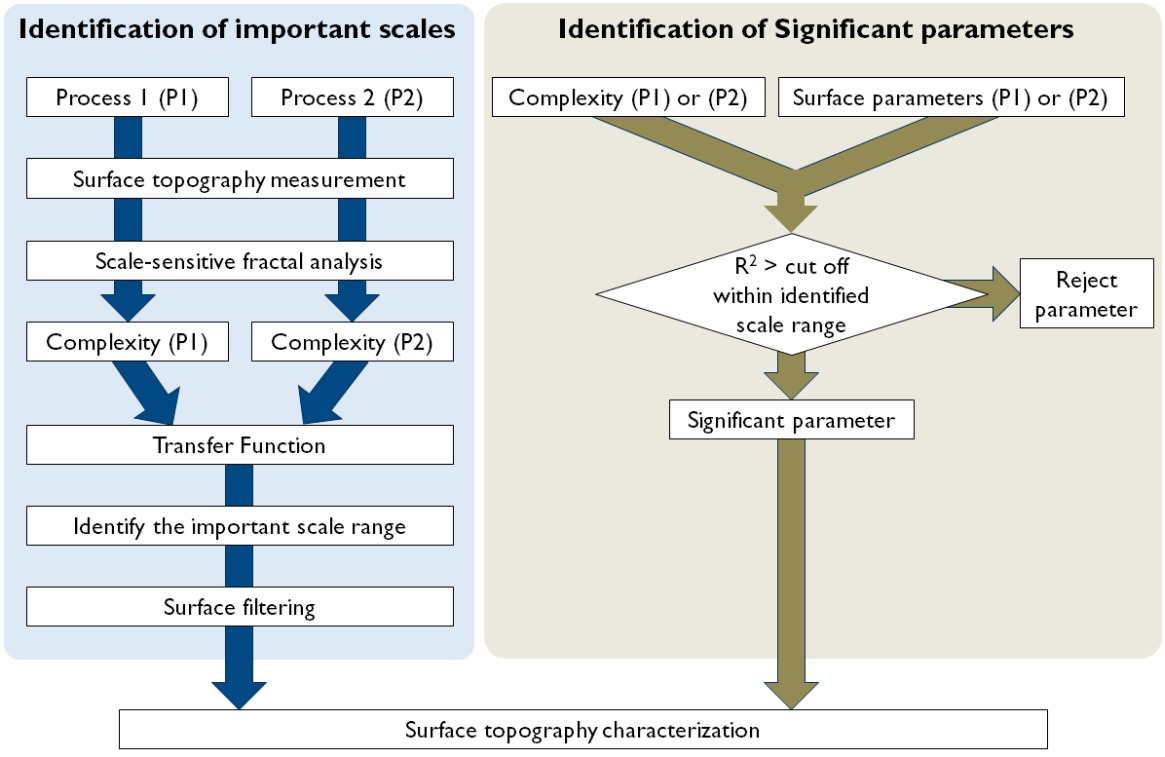

Figure 18. *The generalized methodology of identifying significant parameters for multi-scale surfaces.*

Although the statistical approach is embedded in this method, the final selection of significant parameters is based on “Transfer function” – complexity plot and due to this reason, it is considered as an approach to identify the significant parameters using advanced characterization technique. In scenarios where two processes are to be compared, then this method works effectively and in cases where there are several independent variables are involved then the aforementioned method works best.

6 RESULTS AND DISCUSSION

In the following section, the main results from the appended papers are summarized to answer the research questions. The research questions are framed around the three facets of the surface control loop addressing how the developed research methodology can characterize the additive manufactured surfaces effectively. This is mainly to have an increased understanding of the manufacturing process, thereby providing guidelines for process optimization to enhance surface quality. A summary of the structure of research questions and relevant papers is provided in figure 19. The results from each paper are structured to answer respective research questions.

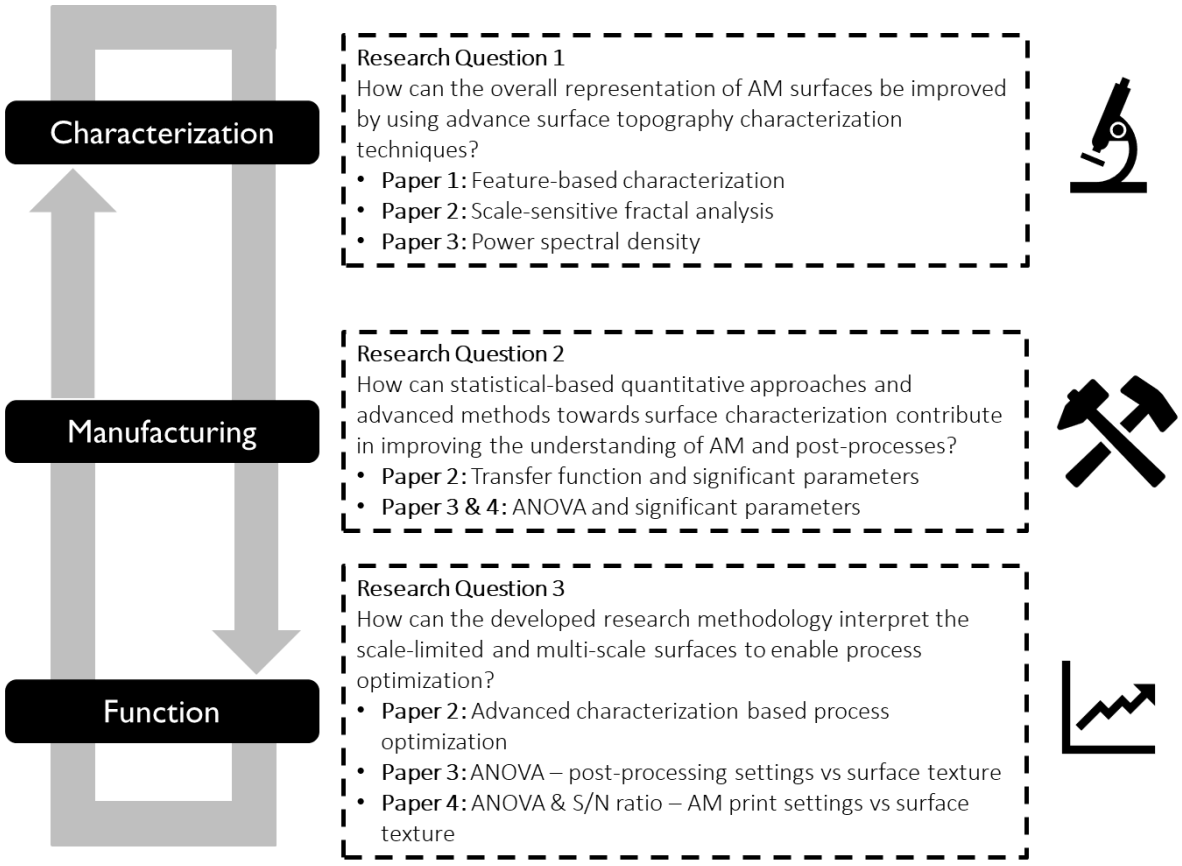

Figure 19. *Overview of research questions*

6.1 Paper 1 – Feature-based characterization of SLM surfaces

In this paper, importance was given to characterize the surface topography of Selective Laser Melting (SLM) parts using feature-based characterization method. The focus of this paper is to characterize the SLM surfaces in a better way than the existing methods to improve the understanding of the manufacturing process. Investigations were carried out on the 316L stainless steel SLM samples. To encounter most of the surface conditions, a truncheon test artefact [102] was utilized for analysis. Figure 20 shows the truncheon artefact with varying build inclination from 0° to 90° in steps of 3° increment. This sample was fabricated using an EOS M290 SLM machine with standard process settings and layer thickness was maintained at 20µm. The steel powders were produced by gas atomization process with the size distribution of 20 to 53µm.

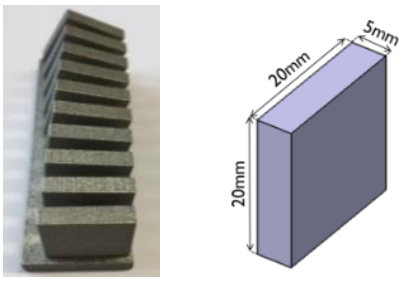

Figure 20. *Truncheon artefact*

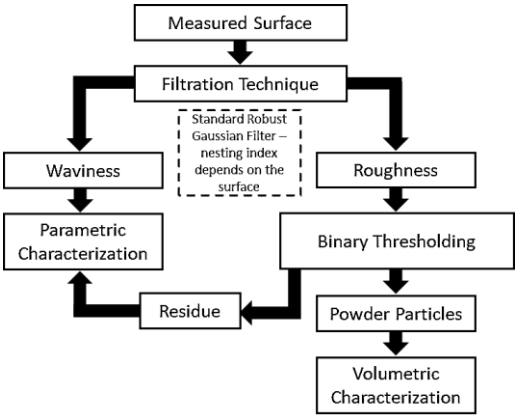

Figure 21. *Complex AM surface characterization strategy.*

A Stylus Profilometer was employed for capturing the areal surface topography of SLM samples. A methodology was developed (see figure 21) to extract and characterize the topographic features of Additive Manufactured (AM) surfaces. Figure 22 shows the images of surface features segregated from the original topography of the SLM sample as per the methodology. The waviness surface includes the "stair-step" effect caused by the build inclination and also the form due to thermal conditions (shrinkages or swelling effects) during the build. The roughness surface obtained includes partially melted powder particles and additional footprints of the process. The roughness surface was further processed to remove the powder particles and the remaining surface is termed as residual surface. The waviness surface (fig. 22b) and residual surface (fig. 22e) were subjected to characterization by areal surface texture parameters (ISO 25178-2) and powder particles (fig. 22d) were quantified volumetrically.

It can be witnessed from figure 23, that the as-built average surface roughness (Sa – original) increases with increase in build inclination, which is a direct contradiction to the proposed model of Reeves and Cobb to predict the average roughness [103]. Equation 5 represents the model built on the concept of stair-step effect in AM to predict average roughness.

$$Ra = \frac{Lt}{4} cos\alpha \tag{5}$$

Where Lt is layer thickness and α is the build inclination.

The extracted waviness surface as per the methodology has a surface roughness (Sa – waviness) trend similar to the model roughness (Ra – model) indicating the presence of a stair-step effect.

This waviness surface represents an ideal situation where all the powder particles have completely melted to build the part during the fabrication process of SLM. However, in reality, some powder particles partially melt, and the surrounding loose powders in the powder bed adhere to the surface during the SLM process, thereby, increasing the surface roughness.

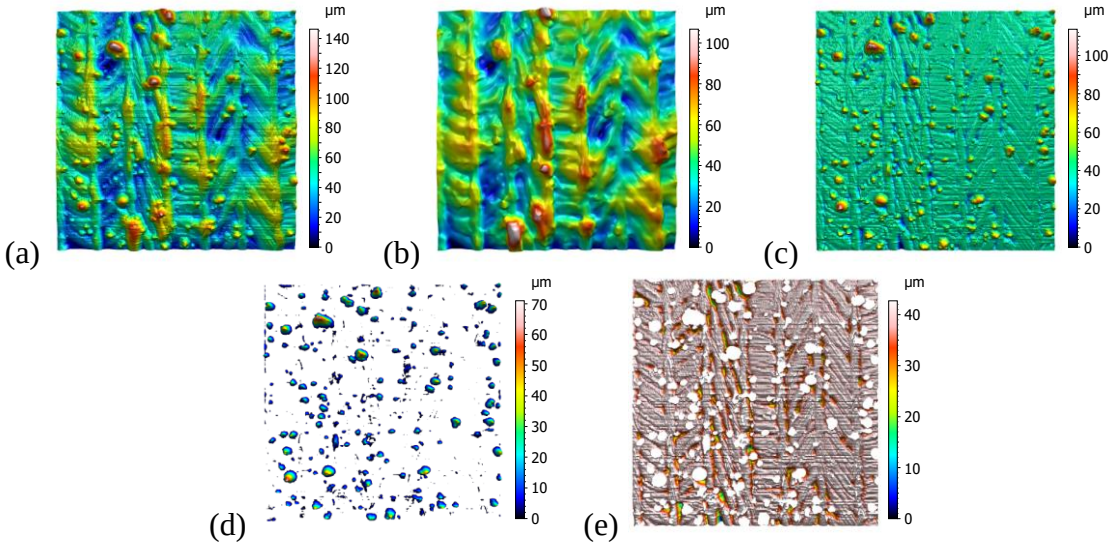

Figure 22. *Isolation of powder particles and staircase effect by applying the Robust Gaussian filter. (a) Original surface (b) Waviness surface (c) Roughness surface (d) Powder particles (e) Residual surface. Measurement area of the captured surface is 2.5mm × 2.5mm.*

The adherence of powder particles to the surface increases with an increase in build inclination since the higher the slopes, the higher will be the contact with powder particles. It can be witnessed in the volume curve of the powder particles in figure 24. After separation of powder particles from the residual surface, as a rule of thumb, the higher the volume of the powder particles, the lower the roughness of the residual surfaces and vice versa. It can be seen from figure 24 that the transition takes place between 6-9˚ build angles, beyond which the powder particles start to dominate the surface. This also implies that at lower build inclination (less than 6°), the stair-step effect is dominant on surface topography, between 9° to 15° there is an increased dominance of powder particles along with the slight effect of stair-stepping, but beyond 15° the methodology used in this study fails to identify the residual surface since it is completely dominated by powder particles.

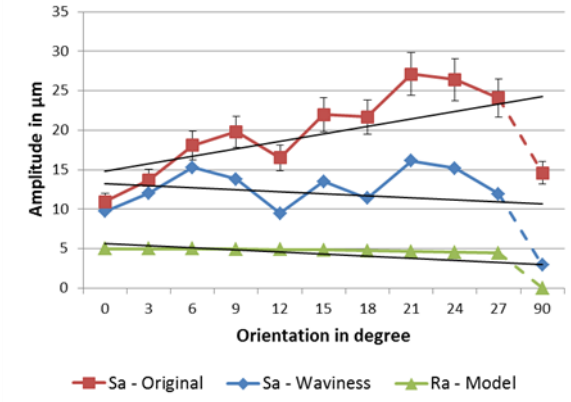

Figure 23*. Average roughness curve*

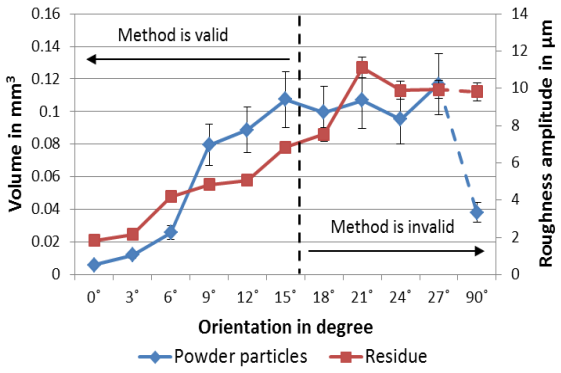

Figure 24*. Volume curve of the powder particles and Sa of residue plotted against the build orientation.*

6.2 Paper 2 – Area-scale analysis & significant parameters

This paper also focuses on having a better understanding of the Laser-Based Powder Bed Fusion of Metals (PBF-LB/M) process to enable optimization through surface analysis. For this purpose, a truncheon artefact [102] was utilized as shown in figure 25. Two sets of samples were produced using identical settings, one set was subjected to shot blasting and the other was retained without any physical modifications (as-built). For ease of analysis, a limited number of surfaces, representing the whole data set, were captured using Confocal Fusion technology. The data were processed to remove the form and measurement noise. The area-scale analysis, a multi-scale approach was utilized to discriminate various surfaces and to understand the influence of design variations and shot blasting characteristics/process parameters on the surface topography of PBF-LB/M parts at various scales. The developed methodology (see section 5.1.2, figure 18) was utilized to identify the most important scale and parameters for characterization.

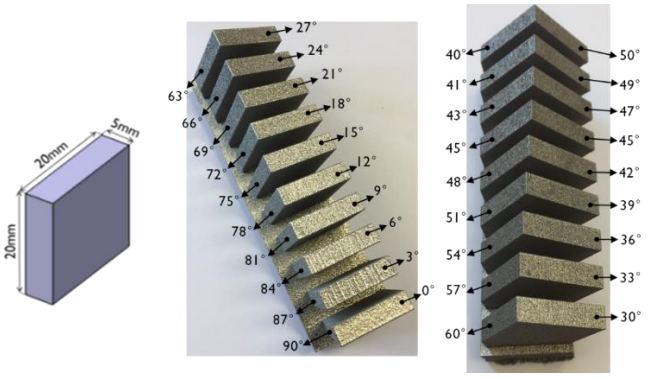

Figure 25. *Truncheon artefact with varying build inclination.*

In the area-scale analysis, complexity plots provide the rate of change of surface intricacy of SLM samples at each scale. The "transfer function" of complexity plot is simply the ratio of complexity plots of as-built and shot-blasted surfaces for all build inclinations. The resulting graph provides information on the effects of blasting over the as-built surface conditions at each scale. The transfer function – complexity plot as shown in figure 26 identifies three importance scales of observation. At mid/intermediate scale range, a significant peak can be observed, indicating a huge difference between shot blasted and as-built surface topography. At smaller scale range, complexity values reach unity indicating that the surface features are similar in both as-built and shot blasted conditions. The large-scale region corresponds to the waviness region containing the stair-step effect. It can be noticed that the waviness varies chaotically at the largest scale, this may be due to the deformations caused by thermal effects (shrinkages and swelling effect) resulting in a non-deterministic pattern on the surface. To further interpret the surface behavior, it is important to consider visual and parametric characterization.

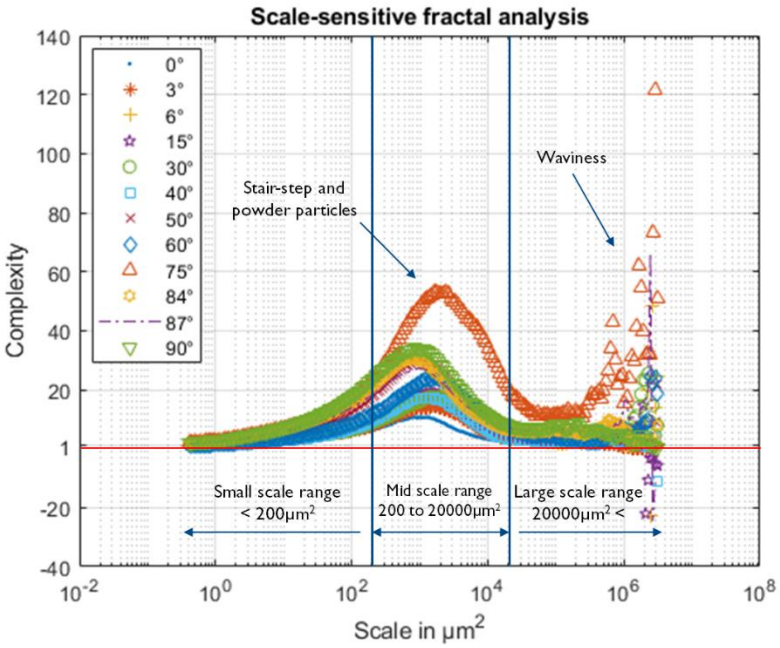

Figure 26. *Transfer function – complexity plot of the PBF-LB/M surfaces at various build inclinations*

The methodology developed allowed to identify the most significant parameters within three important scales of observation. Figure 27 shows areal surface texture parameters such as Sa, Sq, Smc, Vmc, Vvc and Vv have high correlation within the large-scale ranges indicating that the values of these parameters are determined by the waviness of the surface topography. Parameters such as Sdr, Sdq, Sal and Str have a high correlation in the small and intermediate scales. It is important to filter the surfaces with respect to the three identified regions and use corresponding significant parameters to fully understand the effects of post-processing.

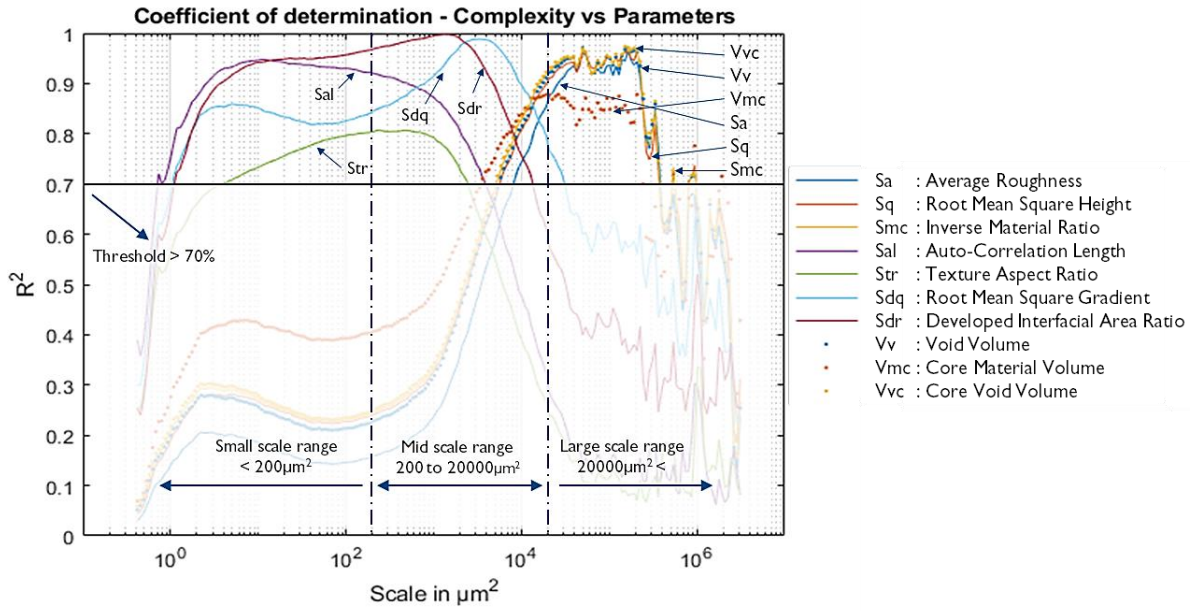

Figure 27. *Coefficient of determination (R^2) of significant parameters obtained by taking correlations between the complexity values and areal surface texture parameters at every scale.*

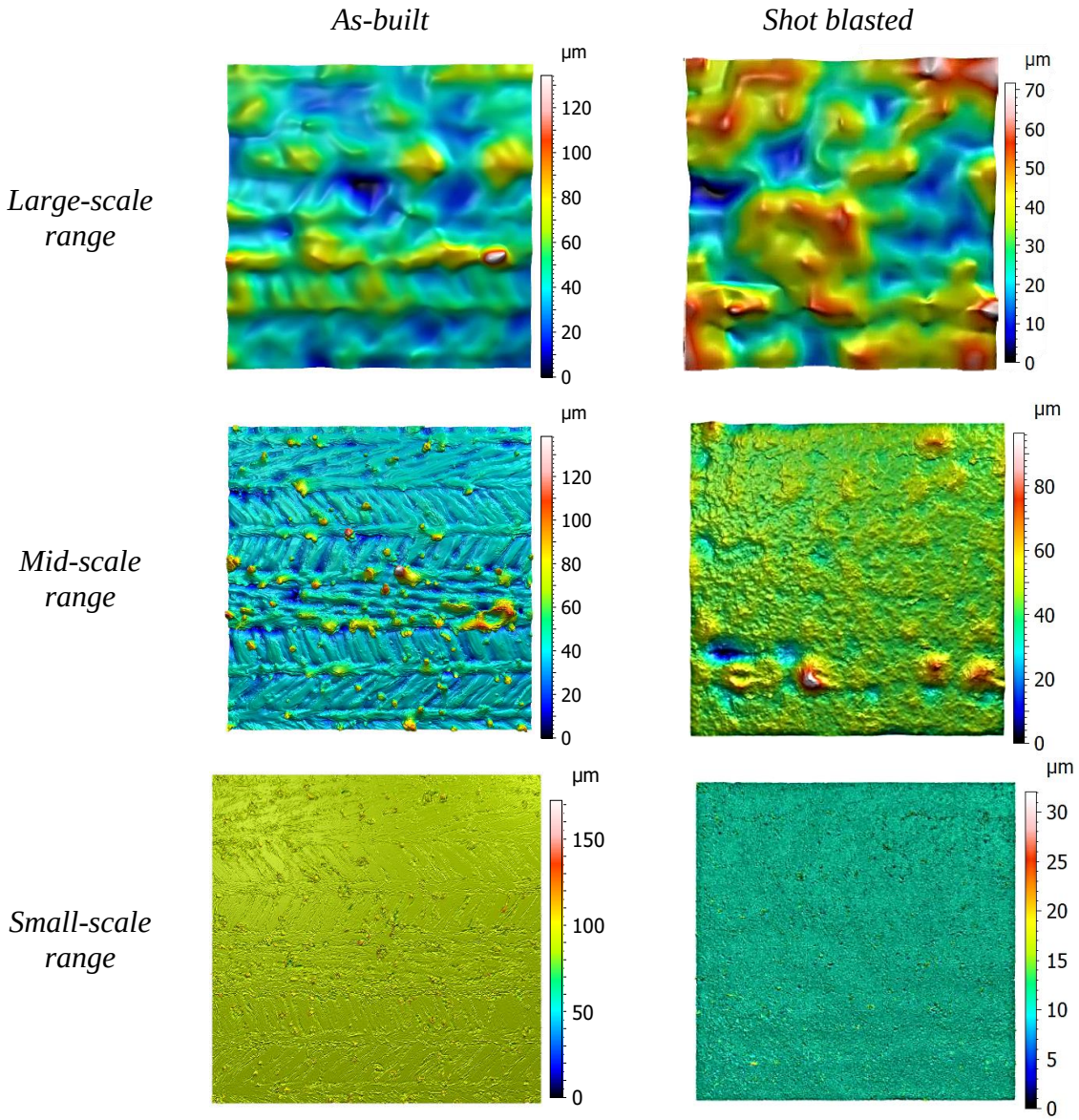

Figure 28. *Filtered surface topography of as-built and shot blasted sample at 3° build inclination for large, mid and small scale ranges. Measurement area was maintained at 2.5mm × 2.5mm.*

From the developed methodology it can be understood that:

- Shot blasting has an insignificant effect on surface features corresponding to the largest scales as it cannot remove the waviness successfully, it can be witnessed in figure 28. Hence, the surface features are similar in both as-built and shot blasted samples, which is also verified by Sa values shown in figure 29a. Therefore, shot blasting may not be recommended for finishing the parts for high-end precision applications. The average roughness (Sa) increases with a decrease in build inclination and usually has the highest roughness at lower build inclinations (less than 15°). Hence, it is recommended to avoid orienting the object with these build inclinations.
- At intermediate scales, the hybrid parameter, Sdr representing the surface intricacy, increases with an increase in build inclination for as-built conditions (see figure 29b). This is due to the increased presence of powder particles at higher build inclinations. However, for shot-blasted surfaces, the Sdr value remains the same for all the build inclinations

indicating that this post-process eliminates both the stair-step effect and powder particles effectively (see figure 29b, mid-scale range). It may be noted that as-built surfaces at lower build inclinations may not need extensive blasting as required by the surfaces at higher build inclinations. Blasting time can be varied based on the type of surface to get the best quality.

- At smaller scales, as-built surfaces exhibit a slight directionality only at lower build inclinations which were completely removed by the blasting process since the shot blasted surfaces exhibit high isotropic property for all the build inclinations. The footprints of shot-blasting due to the abrasive action at finer scales were evident visually (see figure 28, small-scale range – shot-blasted surfaces) but no significant effect in the parameter readings was observed. Further investigations are required.

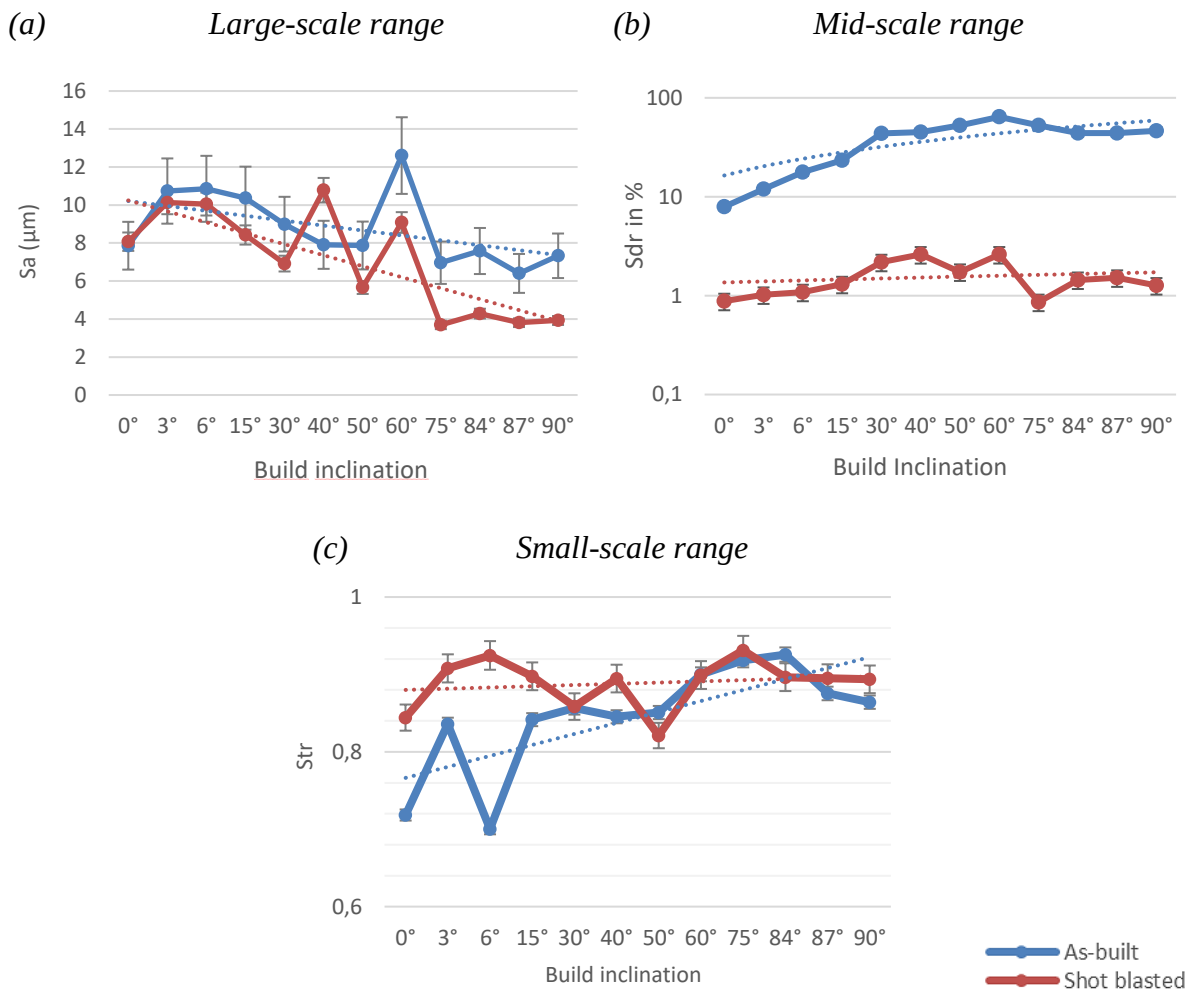

Figure 29. *Variation of selected significant parameters with respect to build inclination in corresponding scale ranges.*

6.3 Paper 3 – Significant parameters using the statistical method and PSD

One of the major challenges with Fused Deposition Modeling (FDM) is its inconsistency in delivering high-quality products and hence, in most cases, it is still being utilized for producing functional prototypes. This paper focuses on enhancing the surface quality of FDM parts by subjecting it to Acetone vapor deposition (AVD) smoothening, Shot-blasting and Laser engraving post-processing methods. A comparative study was presented in this paper, where surface produced by different post-processing methods were compared to the reference injection molding components. The injection molded parts produce a fine and matte surface finish and it is necessary for FDM surfaces to achieve that standard. A methodology was developed to firstly, use multiple regression, a statistical approach for identifying the most significant profile roughness parameter for characterization and to understand the relationship between various post-process settings and surface texture. Secondly, the established knowledge from experiments is implemented on a real industrial product and Power Spectral Density (PSD), advanced characterization approach is employed to discriminate the surfaces.

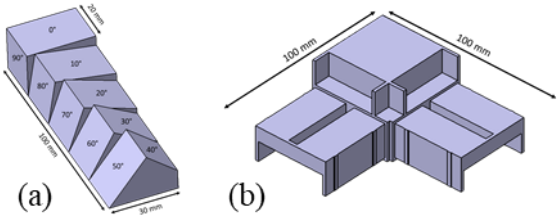

Figure 30. *CAD models of (a) Truncheon artefact and (b) TylöHelö sauna corner knot.*

A truncheon artefact [102] and an industrial product are used for the experiments as shown in figure 30. Stylus profilometer and GFM MikroCAD fringe projection optical microscope are used to capture profile and areal surface texture respectively. A Taguchi's orthogonal array [104] Design of Experiments (DOE) was utilized for each of the post-processing methods to establish an optimized number of tests and regression analysis was employed to investigate the interaction between the process control variables and surface texture. The process control variables for laser-assisted finishing were, laser power, laser speed and resolution; for shot blasting, it was blasting time and blasting media and for Acetone smoothening process, it was exposure time. As per the regression methodology (see section 5.1.1, figure 17), the significant profile parameters that were found common to all the post-processing methods were Rp, Rz and Rdc. Maximum peak height, Rp, was considered to be more relevant in explaining the effects of post-processing variables on surface texture.

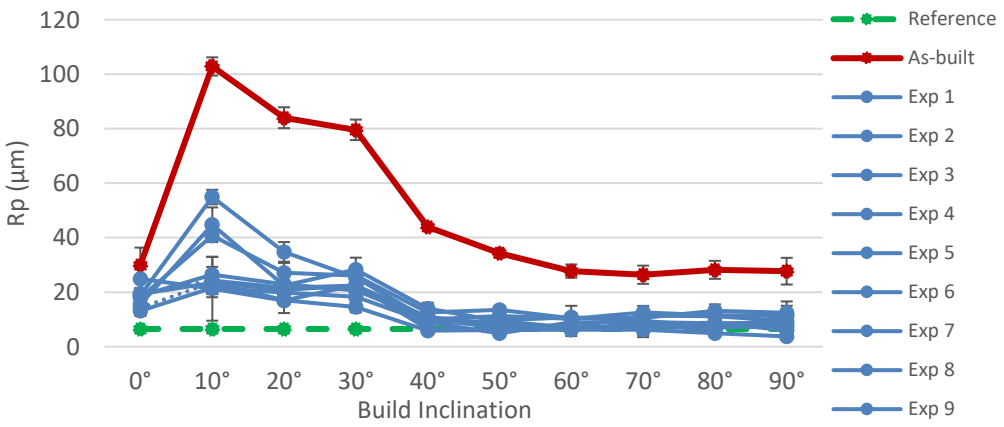

Figure 31. *The maximum peak height of laser finished FDM surface at various build inclination along with as-built and reference injection molding measurements.*

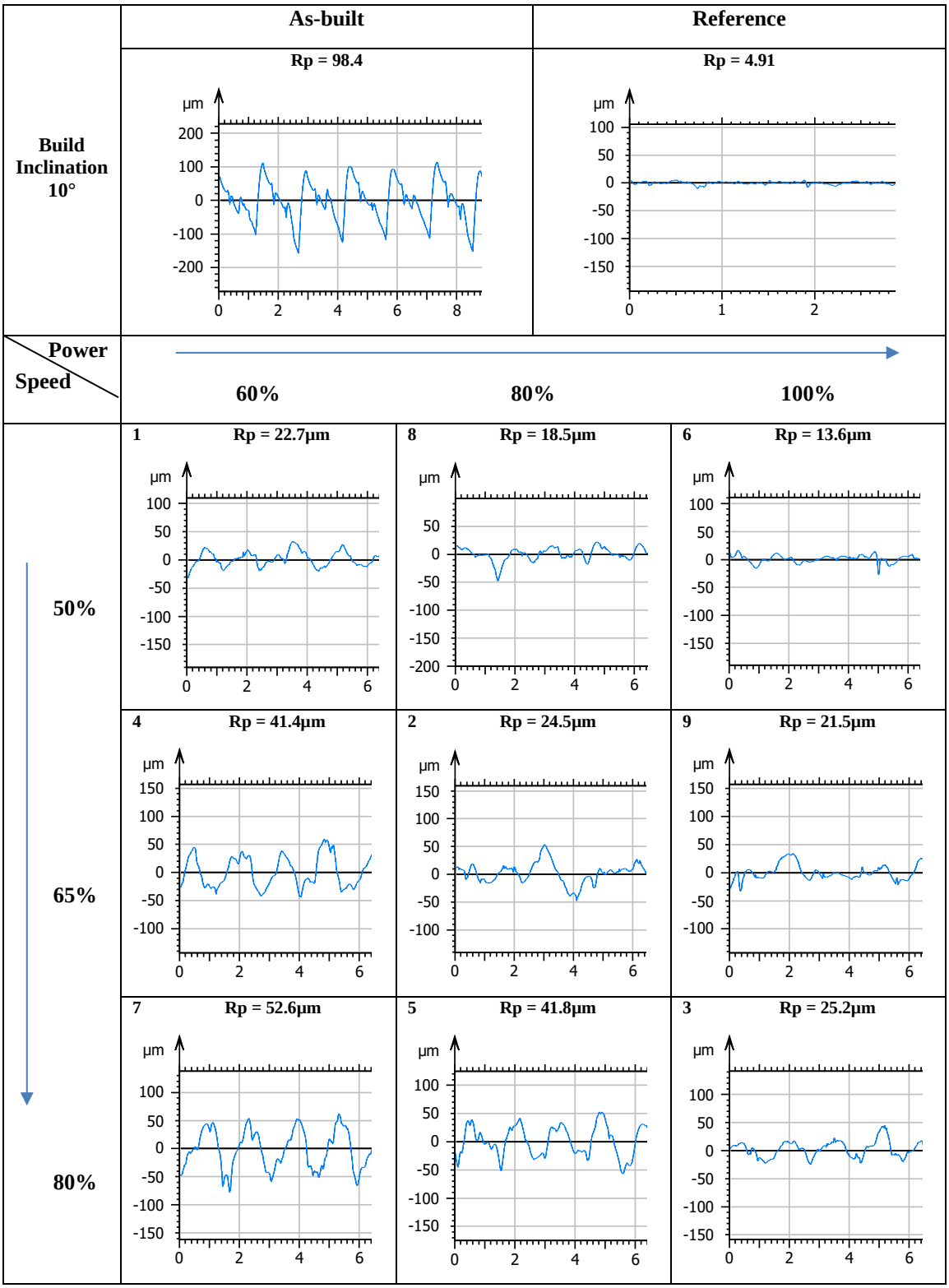

Figure 32. *Profile measurements*

Figure 31 shows the variation of Rp parameter with respect to build inclination for as-built, reference (Injection Molding), and laser finished surfaces as per the different experiments in DOE. It can be noticed that the laser-assisted finishing has drastically reduced the roughness of as-built conditions, however, it failed to produce the roughness similar to the reference injection molding for lower build inclinations (10°, 20° and 30°). For higher build inclinations, the

surfaces produced by laser finishing are close to the reference. From profile measurements in figure 32, it was found that Rp decreases with an increase in build inclination and laser power, and increases with an increase in laser speed. The resolution had a negligible effect on the Rp parameter. Similarly, for shot blasting, blasting time was found to be a more dominant effect on the surface quality than the blasting media and for Acetone vapor deposition process, exposure time had a significant effect.

Although the post-processing methods significantly reduced roughness, they still produced surfaces that were aesthetically hindered. Laser-assisted process ignited the surfaces during melting, leading to discoloration of the part, Shot-blasting was very aggressively damaging the parts and acetone process produced surfaces with a high gloss finish. As a solution, the post-processing methods were combined to achieve both good and aesthetically pleasing surface finish. Nonetheless, none of the post-processing methods managed to eliminate the waviness due to the stair-step effect without damaging the part. Furthermore, the best post-processing method and settings were implemented on the industrial part and were subjected to analysis. Figure 33 shows, the PSD of surfaces produced by post-processing, as-built and reference of industrial product for comparison. It can be noticed that features below the wavelength of 100 are similar in all of the surfaces and the most important difference can be noted in higher wavelength region. The surface features where the difference is at its maximum is filtered to identify the actual difference between different processes. Figure 34 shows the industrial product in as-built, reference injection molding and post-processed conditions, along with surface topography before and after filtering the most critical features. It can be seen that acetone+blasted surfaces have a better finish than the injection molding samples. Laser+blasting has surface roughness closer to as-built conditions, however, the strong directionality of as-built surfaces was completely removed. Acetone process can only work with samples that are reactive to it, in other cases laser process can be found beneficial.

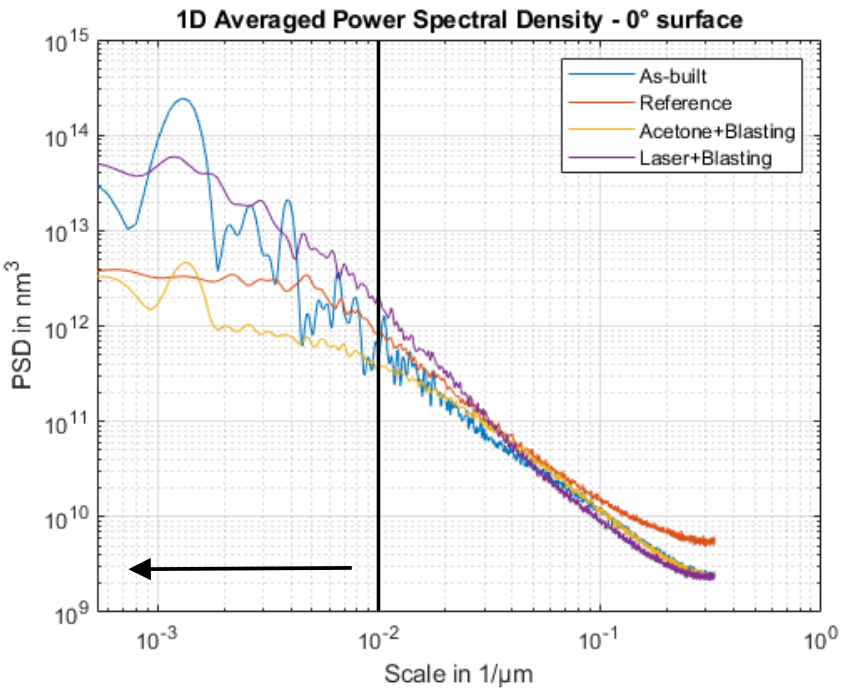

Figure 33. *One dimensional averaged power spectral density of As-built, Reference injection molding, Acetone+Blasting, Laser+Blasting surfaces at 0° build inclination.*

In conclusion, this paper provided a statistical tool for quick assessment of surface quality and to understand the effects of post-processing variables on surface texture. Based on the experiments, post-processing methods and settings were optimized to get a good finish to the final end-product. Finally, an advanced characterization tool was utilized to further pin-point the surface features that revealed the maximum difference in the various processes.

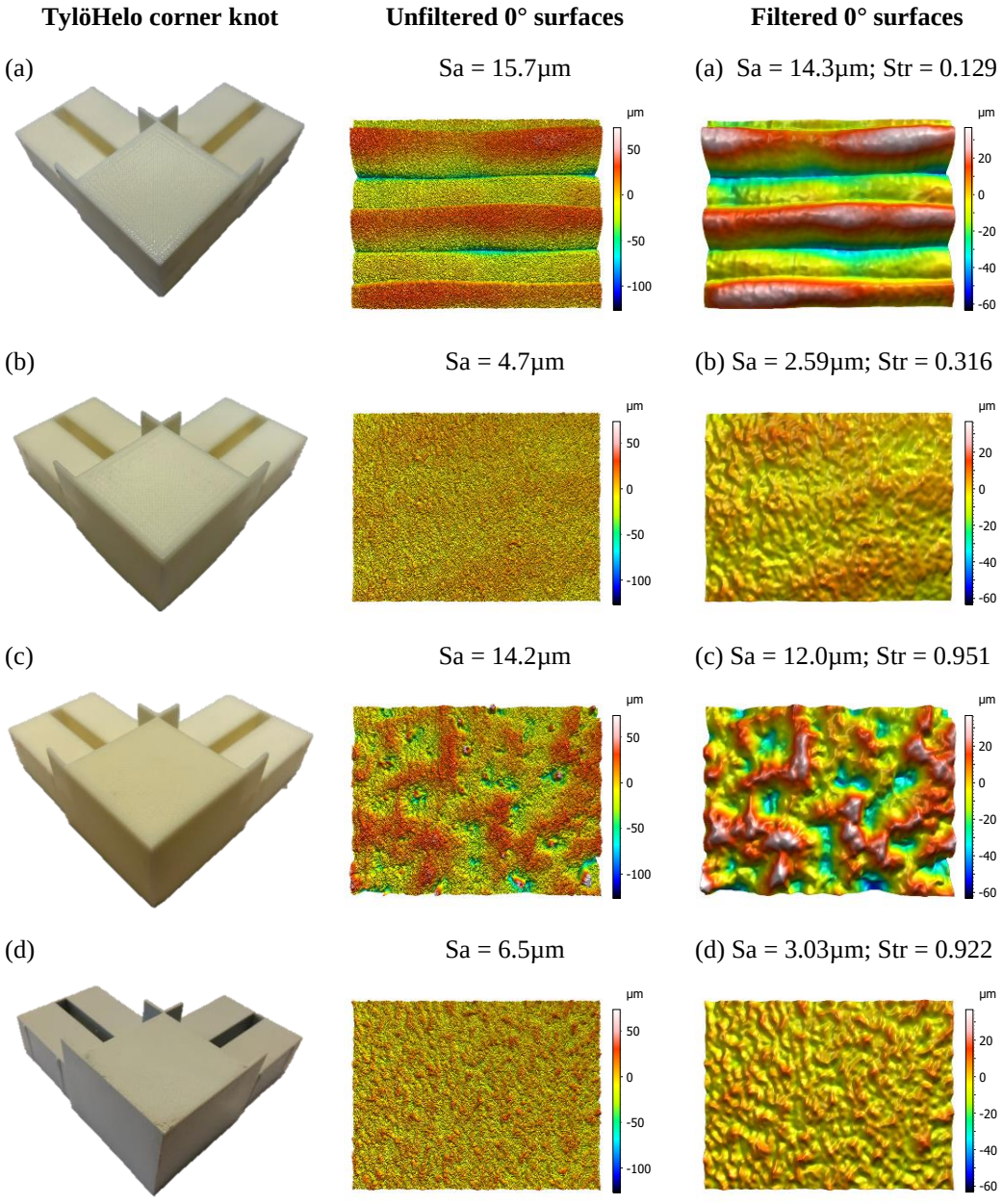

Figure 34. *TylöHelo sauna corner knot with unfiltered and filtered surfaces (a) As-built FDM surface (b) Acetone + glass blasted surface (c) Laser + glass blasted surface (d) Reference injection molding surface. Measurement area of the captured surfaces is 2.5mm × 2.5mm.*

6.4 Paper 4 – Significant parameters using statistical methods and S/N ratio

In the previous section, the focus was on using a linear statistical approach to characterize the FDM surfaces and to understand the influence of post-processing settings on surface texture. In this paper, the focus is on interpreting the effects of FDM print settings on surface texture. Investigations were conducted on a truncheon artefact with varying build inclinations from 10° to 90°. Taguchi's orthogonal array design of experiments [104] was utilized to produce an optimized number of experiments required for the study. Truncheon artefact [102] was fabricated as per the DOE containing varying layer thickness, print quality (print speed) and material infill. Quantitative surface texture measurements by Stylus profilometer were made to obtain 2D profile roughness parameters to characterize the FDM surfaces. The profile roughness parameters were linearly regressed with process control variables to study its effects on surface quality and also to find the most significant profile parameters for characterization. In addition, the signal to noise ratio (S/N) was used to quantify the influence of FDM process variables on significant parameters.

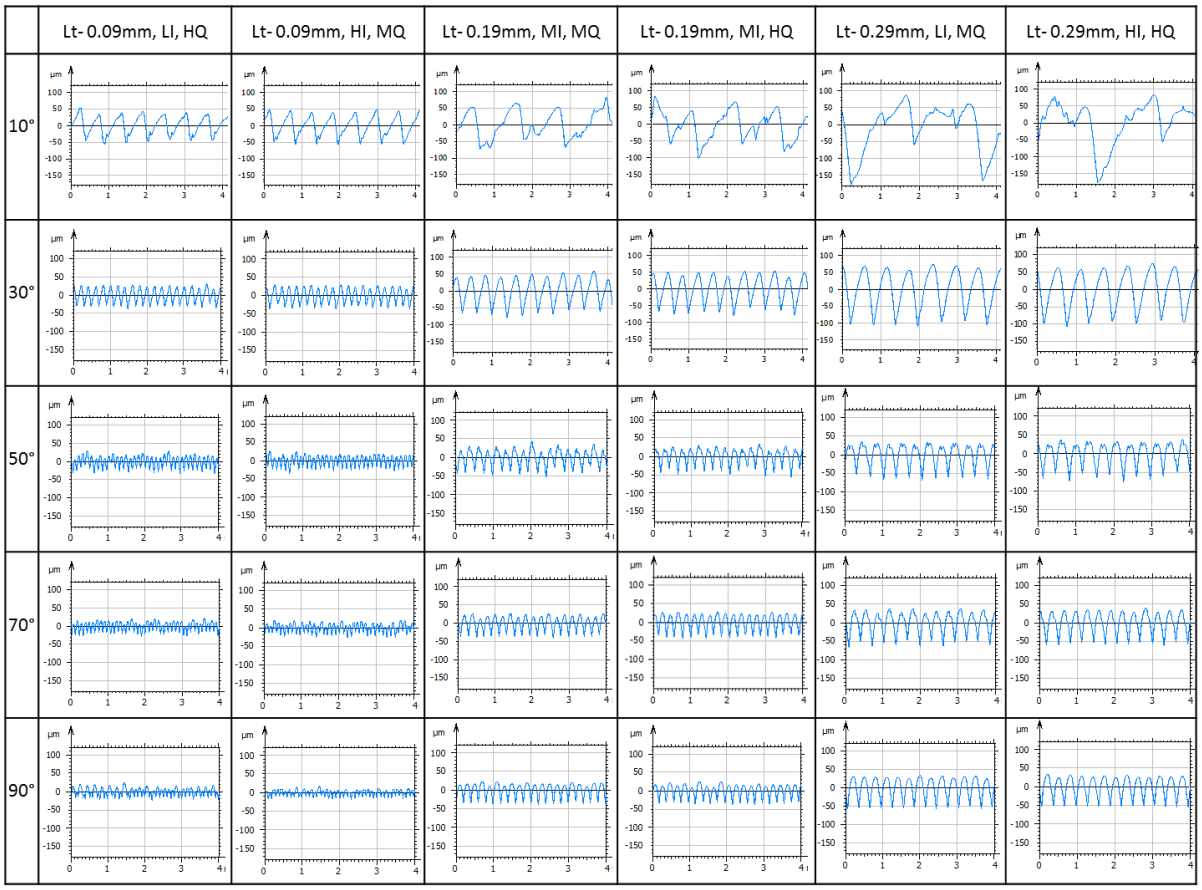

***Figure 35**. Roughness profile measurements*

The results suggest that profile roughness parameters such as Rp, Rv, Rz, Ra, RSm, Rdc and Rpc were found to be significant for the study. All of these significant parameters value except Rpc decreases with an increase in build inclination and increases with an increase in layer thickness. The opposite behavior can be observed with Rpc parameter. This result suggests that when the build inclination increases, amplitude and spacing of the roughness profile decrease, thereby, increasing the number of stair-steps. When layer thickness increases, amplitude and spacing increase, reducing the number of stair-steps. This can be observed from the profile measurements shown in figure 35 and parameter readings in figure 36. Material infill and print quality were found to have an insignificant effect on surface texture.

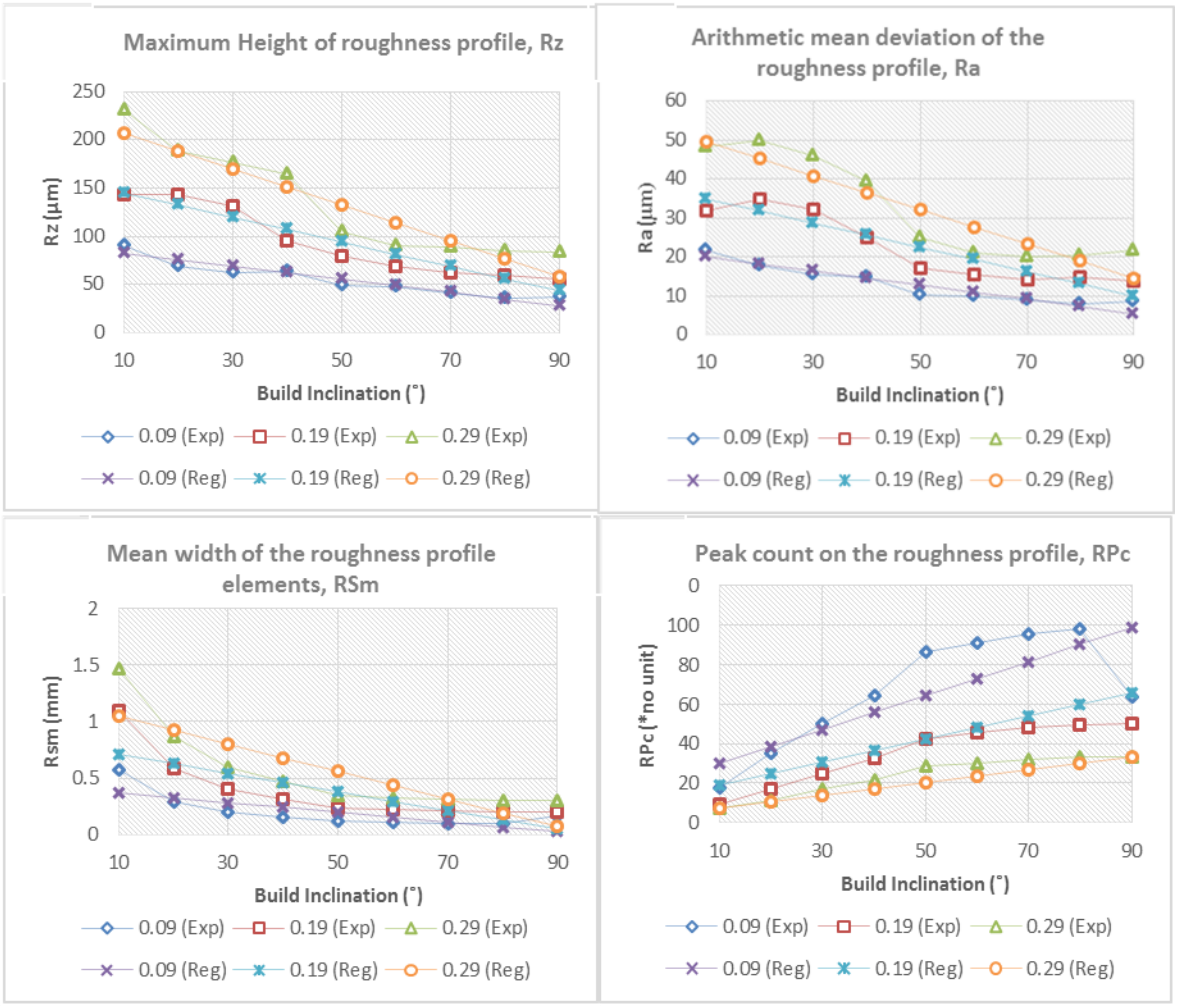

Figure 36. *Mean and predicted values of significant- amplitude and spacing parameters.*

Signal-to-noise ratio results suggested that build inclination had a higher effect for parameters Rpc and Rsm than any other process variables, as shown in figure 37. It can be witnessed visually from figure 35 & figure 36, that the rate of change of peak counts and spacing (Rpc & Rsm) is more with the change in build inclination than the change in layer thickness. For instance, if profiles of 10° and 90° are compared for a single layer thickness, the rate of change of profile curves and values of Rpc and Rsm is higher than the comparison between the change in layer thickness (0.09 to 0.29 mm) for a single build inclination. S/N ratio can be useful in identifying which process variable has the most influence on surface quality.

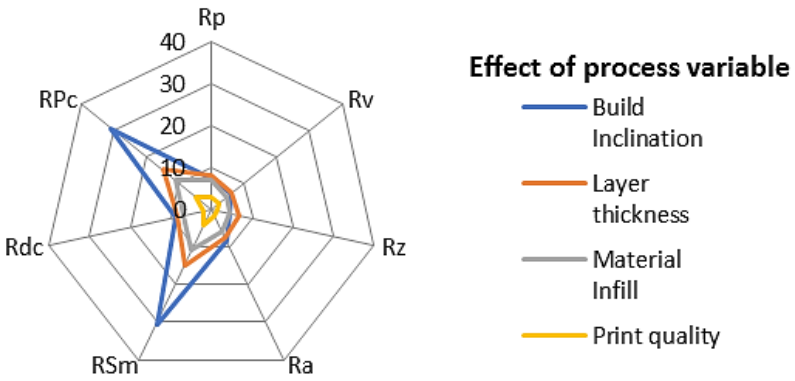

Figure 37. *Signal to noise ratio of significant parameters*

7 CONCLUSIONS AND FUTURE WORK

7.1 Conclusions

Additive Manufacturing has proven to have the potential to be the next generation of technology in part manufacture. Therefore, the focus has been shifted towards making AM process more robust and reliable for its widespread adoption in industries. One such attempt is made in this thesis by providing guidelines to AM users for process optimization through surface analysis. This thesis provides several potential approaches to characterize the complex AM surfaces with a primary purpose to improve the surface quality and its functional behavior. Diversity in this research concerning AM technologies, surface metrology and characterization techniques along with statistical approaches provides a strong foundation for researchers and manufacturers aiming to improve the surface quality. The study can be summed up by answering the following research questions.

RQ1: *How can the overall representation of AM surfaces be improved by using advanced surface topography characterization techniques?*

The study on the surface topography of AM samples has predominantly been based on profile measurements, which often do not fully reflect the functional behavior. Characterization by areal surface texture parameters (ISO 25178-2) is effective, however, most of these parameters are a direct counterpart of profile parameters (ISO 4287) and average parameters are mostly used for surface description. This emphasizes the need for advanced characterization methods. It can help in mapping the measured surface topography at various scales of observation and as a function of spatial frequency which can be useful to extract the most crucial surface features. Characterizing these features not only strengthens the correlation between the surface and functional performance of the part but also improves the overall representation of AM surfaces. The papers 1, 2 and 3 portray the use of advanced methods such as Feature-based characterization, Scale-sensitive fractal analysis using area-scale relations and Power Spectral Density. The contrast between direct quantification of surfaces via texture parameters and using advanced methods in combination with texture parameters has been displayed in these papers.

RQ2: *How can statistical-based quantitative approaches and advanced methods towards surface characterization contribute to improving the understanding of AM and post-processes?*

In most of the published research, the quantification of as-built and post-processed AM surfaces are based on Ra or Sa, average roughness parameters, which provides a limited understanding of the manufacturing process since it does not provide a complete description of the surface under inspection. The effective representation of surface topography is crucial in understanding the manufacturing process. This thesis provides a technique to identify the most significant surface/profile roughness parameters representing the “footprints” on the surface, unique to each manufacturing process. Analyzing these unique features on the surface topography can lead to an enhanced understanding of the manufacturing process.

Multiple regression statistical approach was used to analyze the measured surface with respect to two or more independent variables at a particular scale and the most significant parameters were the ones that had the highest adjusted coefficient of determination (adj. R^2) value. Similarly, advanced approach by area-scale analysis examined the measured surface at various scales of observation and the most significant parameters were the parameters with high R^2 value within the identified scale of interest as per the “Transfer function” plot.

RQ3: *How does the developed research methodology interpret the scale-limited and multi-scale surfaces to enable process optimization?*

Surface interpretation is crucial in having enhanced manufacturing process control and to attain stability in the essential physical processes to achieve the desired surface quality and functional performance of the part. The developed research methodology in this thesis can not only be used for the identification of significant parameters but also to identify the influence of various process variables (independent variables- AM or post-process settings) on the surface texture. This enables process optimization where the process settings can be adjusted as per the requirements to get the desired outcome.

For scale-limited surfaces, multiple regression statistical method was employed to identify the influence of AM print settings (layer thickness, print temperature, infill settings and so on) and post-process settings (shot-blasting, laser-finishing and acetone process settings) on surface topography. Besides, the signal-to-noise ratio was utilized for determining which process variable had a dominant effect on surface texture. By understanding this relationship, it is possible to vary or adjust the settings of a particular manufacturing process to achieve the desired results. Similarly, for multi-scale surfaces, advanced characterization technique by area-scale analysis was utilized to identify the critical surface features and for interpreting the influence of process variables on surface texture at different scales. This method works best while comparing two processes (as-built and shot-blasted surfaces) with limited process variables.

Multiple regression was mainly focused on scale-limited surfaces to bring out the overall differences in manufacturing processes and to have a general understanding of how various factors affect the surface texture. The area-scale analysis was employed for bringing out more focused differences in processes by analyzing surfaces at different scales and to identify which surface features gets affected the most by process variables.

7.2 Future work

The current scope of this thesis is to have an effective characterization of surface topography of Additive Manufactured surfaces thereby increasing the understanding of its process and providing inputs for process optimization to produce parts with enhanced surface quality and function. Future work involves reducing the gaps identified in this thesis and also to verify the accuracy of the established methods and results.

It is important to explore other surface measurements techniques and characterization methods to quantify the surfaces in general and also to describe the re-entrant surface features in AM. The statistical methodology employed in this thesis uses a linear approach to establish the relationship between the dependent and independent variables, however, it is necessary to explore the polynomial model to verify the usefulness of this approach. Furthermore, the correlations between surface texture and functional behavior have to be explored. Although the developed methodology predicts the functional behavior of the surface under inspection, it is required to verify to fully establish the correlation between them. It could be of great importance to compare the developed research approach with the existing methods for characterizing AM surfaces. In doing so, it is possible to estimate the amount of impact that the developed approach has in predicting the functional performance of the part. Furthermore, this can provide a valuable addition to the surface quality guideline for AM manufacturers who are looking to maximize the surface quality and function of the parts produced.

REFERENCES

[1] I. Gibson, D. Rosen, and B. Stucker, *Additive Manufacturing Technologies*. New York, NY: Springer New York, 2015.

[2] M. Wiese, S. Thiede, and C. Herrmann, "Rapid manufacturing of automotive polymer series parts: A systematic review of processes, materials and challenges," *Addit. Manuf.*, vol. 36, p. 101582, Dec. 2020, doi: 10.1016/j.addma.2020.101582.

[3] A. Gisario, M. Kazarian, F. Martina, and M. Mehrpouya, "Metal additive manufacturing in the commercial aviation industry: A review," *Journal of Manufacturing Systems*, vol. 53. Elsevier B.V., pp. 124–149, Oct. 01, 2019, doi: 10.1016/j.jmsy.2019.08.005.

[4] M. A. Ali, M. Rajabi, and S. Sudhir Sali, "Additive manufacturing potential for medical devices and technology," *Current Opinion in Chemical Engineering*, vol. 28. Elsevier Ltd, pp. 127–133, Jun. 01, 2020, doi: 10.1016/j.coche.2020.05.001.

[5] R. Galante, C. G. Figueiredo-Pina, and A. P. Serro, "Additive manufacturing of ceramics for dental applications: A review," *Dental Materials*, vol. 35, no. 6. Elsevier Inc., pp. 825–846, Jun. 01, 2019, doi: 10.1016/j.dental.2019.02.026.

[6] C. J. Bae, A. B. Diggs, and A. Ramachandran, "Quantification and certification of additive manufacturing materials and processes," in *Additive Manufacturing: Materials, Processes, Quantifications and Applications*, Elsevier, 2018, pp. 181–213.

[7] R. Leach, Ed., *Optical Measurement of Surface Topography*. Springer Berlin Heidelberg, 2011.

[8] K. J. Stout and E. J. Davis, "Surface topography of cylinder bores - the relationship between manufacture, characterization and function," *Wear*, vol. 95, no. 2, pp. 111–125, 1984, doi: 10.1016/0043-1648(84)90111-X.

[9] F. Zanini, L. Pagani, P. J. Scott, E. Savio, and S. Carmignato, "Measurement of additively manufactured surfaces with re-entrant features by x-ray computed tomography," *Proc. - 2018 ASPE euspen Summer Top. Meet. Adv. Precis. Addit. Manuf.*, no. July, pp. 222–225, 2018.

[10] "ISO/ASTM 52900:2015(en), Additive manufacturing — General principles — Terminology," Geneva, 2015.

[11] W. E. Frazier, "Metal additive manufacturing: A review," *Journal of Materials Engineering and Performance*, vol. 23, no. 6. Springer New York LLC, pp. 1917–1928, Apr. 08, 2014, doi: 10.1007/s11665-014-0958-z.

[12] S. Yuan, F. Shen, C. K. Chua, and K. Zhou, "Polymeric composites for powder-based additive manufacturing: Materials and applications," *Progress in Polymer Science*, vol. 91. Elsevier Ltd, pp. 141–168, Apr. 01, 2019, doi: 10.1016/j.progpolymsci.2018.11.001.

[13] L. E. Murr *et al.*, "Fabrication of metal and alloy components by additive manufacturing: Examples of 3D materials science," *Journal of Materials Research and Technology*, vol. 1, no. 1. Elsevier Editora Ltda, pp. 42–54, Apr. 01, 2012, doi: 10.1016/S2238-7854(12)70009-1.

[14] S. Cooke, K. Ahmadi, S. Willerth, and R. Herring, "Metal additive manufacturing: Technology, metallurgy and modelling," *Journal of Manufacturing Processes*, vol. 57. Elsevier Ltd, pp. 978–1003, Sep. 01, 2020, doi: 10.1016/j.jmapro.2020.07.025.

[15] S. C. Daminabo, S. Goel, S. A. Grammatikos, H. Y. Nezhad, and V. K. Thakur, "Fused deposition modeling-based additive manufacturing (3D printing): techniques for polymer material systems," *Materials Today Chemistry*, vol. 16. Elsevier Ltd, p. 100248, Jun. 01, 2020, doi: 10.1016/j.mtchem.2020.100248.

[16] S. C. Ligon, R. Liska, J. Stampfl, M. Gurr, and R. Mülhaupt, “Polymers for 3D Printing and Customized Additive Manufacturing,” *Chemical Reviews*, vol. 117, no. 15. American Chemical Society, pp. 10212–10290, Aug. 09, 2017, doi: 10.1021/acs.chemrev.7b00074.
[17] B. N. Turner and S. A. Gold, “A review of melt extrusion additive manufacturing processes: II. Materials, dimensional accuracy, and surface roughness,” *Rapid Prototyping Journal*, vol. 21, no. 3. Emerald Group Publishing Ltd., pp. 250–261, Apr. 20, 2015, doi: 10.1108/RPJ-02-2013-0017.
[18] B. Khoshnevis, “Automated construction by contour crafting - Related robotics and information technologies,” in *Automation in Construction*, Jan. 2004, vol. 13, no. 1, pp. 5–19, doi: 10.1016/j.autcon.2003.08.012.
[19] F. Hamidi and F. Aslani, “Additive manufacturing of cementitious composites: Materials, methods, potentials, and challenges,” *Construction and Building Materials*, vol. 218. Elsevier Ltd, pp. 582–609, Sep. 10, 2019, doi: 10.1016/j.conbuildmat.2019.05.140.
[20] A. Paolini, S. Kollmannsberger, and E. Rank, “Additive manufacturing in construction: A review on processes, applications, and digital planning methods,” *Additive Manufacturing*, vol. 30. Elsevier B.V., p. 100894, Dec. 01, 2019, doi: 10.1016/j.addma.2019.100894.
[21] A. Habib and B. Khoda, “Development of clay based novel hybrid bio-ink for 3D bio-printing process,” *J. Manuf. Process.*, vol. 38, pp. 76–87, Feb. 2019, doi: 10.1016/j.jmapro.2018.12.034.
[22] S. V. Murphy and A. Atala, “3D bioprinting of tissues and organs,” *Nature Biotechnology*, vol. 32, no. 8. Nature Publishing Group, pp. 773–785, 2014, doi: 10.1038/nbt.2958.
[23] J. Malda *et al.*, “25th anniversary article: Engineering hydrogels for biofabrication,” *Advanced Materials*, vol. 25, no. 36. John Wiley & Sons, Ltd, pp. 5011–5028, Sep. 01, 2013, doi: 10.1002/adma.201302042.
[24] C. J. Thrasher, “Advanced Methods and Materials for Vat Photopolymerization Additive Manufacturing,” 2017.
[25] H. Wu *et al.*, “Recent developments in polymers/polymer nanocomposites for additive manufacturing,” *Progress in Materials Science*, vol. 111. Elsevier Ltd, p. 100638, Jun. 01, 2020, doi: 10.1016/j.pmatsci.2020.100638.
[26] F. Li *et al.*, “Digital light processing 3D printing of ceramic shell for precision casting,” *Mater. Lett.*, vol. 276, p. 128037, Oct. 2020, doi: 10.1016/j.matlet.2020.128037.
[27] A. R. Johnson *et al.*, “Single-step fabrication of computationally designed microneedles by continuous liquid interface production,” *PLoS One*, vol. 11, no. 9, Sep. 2016, doi: 10.1371/journal.pone.0162518.
[28] P. Gu, X. Zhang, Y. Zeng, and B. Ferguson, “Quality analysis and optimization of solid ground curing process,” *J. Manuf. Syst.*, vol. 20, no. 4, pp. 250–263, Jan. 2001, doi: 10.1016/S0278-6125(01)80045-5.
[29] J. Y. Lee, J. An, and C. K. Chua, “Fundamentals and applications of 3D printing for novel materials,” *Applied Materials Today*, vol. 7. Elsevier Ltd, pp. 120–133, Jun. 01, 2017, doi: 10.1016/j.apmt.2017.02.004.
[30] M. Ziaee and N. B. Crane, “Binder jetting: A review of process, materials, and methods,” *Additive Manufacturing*, vol. 28. Elsevier B.V., pp. 781–801, Aug. 01, 2019, doi: 10.1016/j.addma.2019.05.031.
[31] S. Yi, F. Liu, J. Zhang, and S. Xiong, “Study of the key technologies of LOM for

functional metal parts," in *Journal of Materials Processing Technology*, Jul. 2004, vol. 150, no. 1–2, pp. 175–181, doi: 10.1016/j.jmatprotec.2004.01.035.
[32] A. Bournias-Varotsis, X. Han, R. A. Harris, and D. S. Engstrøm, "Ultrasonic additive manufacturing using feedstock with build-in circuitry for 3D metal embedded electronics," *Addit. Manuf.*, vol. 29, p. 100799, Oct. 2019, doi: 10.1016/j.addma.2019.100799.
[33] S. M. Thompson, L. Bian, N. Shamsaei, and A. Yadollahi, "An overview of Direct Laser Deposition for additive manufacturing; Part I: Transport phenomena, modeling and diagnostics," *Additive Manufacturing*, vol. 8. Elsevier B.V., pp. 36–62, Oct. 01, 2015, doi: 10.1016/j.addma.2015.07.001.
[34] O. US EPA, "Sustainable Manufacturing," Accessed: Aug. 21, 2020. [Online]. Available: https://www.epa.gov/sustainability/sustainable-manufacturing.
[35] T. Sustainable and D. Goals, "The sustainable development goals report 2016," *Sustain. Dev. goals Rep. 2016*, 2016, doi: 10.29171/azu_acku_pamphlet_k3240_s878_2016.
[36] S. H. Huang, P. Liu, A. Mokasdar, and L. Hou, "Additive manufacturing and its societal impact: A literature review," *International Journal of Advanced Manufacturing Technology*, vol. 67, no. 5–8. Springer, pp. 1191–1203, Jul. 16, 2013, doi: 10.1007/s00170-012-4558-5.
[37] A. Townsend, N. Senin, L. Blunt, R. K. Leach, and J. S. Taylor, "Surface texture metrology for metal additive manufacturing: a review," *Precision Engineering*, vol. 46. Elsevier Inc., pp. 34–47, Oct. 01, 2016, doi: 10.1016/j.precisioneng.2016.06.001.
[38] J. S. Taylor, "Physical processes linking input parameters and surfacemorphology in additivemanufacturing," *ASPE Spring Top. Precis. Toler. Addit.*, pp. 70–1, 2015.
[39] V. Reddy, O. Flys, A. Chaparala, C. E. Berrimi, V. Amogh, and B. G. Rosen, "Study on surface texture of Fused Deposition Modeling," in *Procedia Manufacturing*, 2018, vol. 25, pp. 389–396, doi: 10.1016/j.promfg.2018.06.108.
[40] Stephen Oluwashola Akande, "Dimensional Accuracy and Surface Finish Optimization of Fused Deposition Modelling Parts using Desirability Function Analysis," *Int. J. Eng. Res.*, vol. V4, no. 04, pp. 196–202, 2015, doi: 10.17577/ijertv4is040393.
[41] D. Ahn, H. Kim, and S. Lee, "Surface roughness prediction using measured data and interpolation in layered manufacturing," *J. Mater. Process. Technol.*, vol. 209, no. 2, pp. 664–671, Jan. 2009, doi: 10.1016/j.jmatprotec.2008.02.050.
[42] H. I. Medellin-Castillo and J. Zaragoza-Siqueiros, "Design and Manufacturing Strategies for Fused Deposition Modelling in Additive Manufacturing: A Review," *Chinese J. Mech. Eng. (English Ed.*, vol. 32, no. 1, 2019, doi: 10.1186/s10033-019-0368-0.
[43] R. E. Williams and V. L. Melton, "Abrasive flow finishing of stereolithography prototypes," *Rapid Prototyp. J.*, vol. 4, no. 2, pp. 56–67, 1998, doi: 10.1108/13552549810207279.
[44] K. F. Leong, C. K. Chua, G. S. Chua, and C. H. Tan, "Abrasive jet deburring of jewellery models built by stereolithography apparatus (SLA)," *J. Mater. Process. Technol.*, vol. 83, no. 1–3, pp. 36–47, Nov. 1998, doi: 10.1016/S0924-0136(98)00041-7.
[45] A. P. Nagalingam, H. K. Yuvaraj, and S. H. Yeo, "Synergistic effects in hydrodynamic cavitation abrasive finishing for internal surface-finish enhancement of additive-manufactured components," *Addit. Manuf.*, vol. 33, p. 101110, May 2020, doi: 10.1016/j.addma.2020.101110.
[46] O. FLYS *et al.*, "Heat transfer and flow performance in additively manufactured

cooling channels with varying surface topography," *J. Japan Soc. Precis. Eng.*, vol. 86, no. 1, pp. 71–79, Jan. 2020, doi: 10.2493/jjspe.86.71.
[47] R. C. Mulhall and N. D. Nedas, "Impact blasting with glass beads," *Met. Finish.*, vol. 105, no. 10, pp. 65–71, Jan. 2007, doi: 10.1016/S0026-0576(07)80319-9.
[48] M. Taufik and P. K. Jain, "Laser assisted finishing process for improved surface finish of fused deposition modelled parts," *J. Manuf. Process.*, vol. 30, pp. 161–177, Dec. 2017, doi: 10.1016/j.jmapro.2017.09.020.
[49] E. Yasa, J. Deckers, and J. P. Kruth, "The investigation of the influence of laser re-melting on density, surface quality and microstructure of selective laser melting parts," *Rapid Prototyp. J.*, vol. 17, no. 5, pp. 312–327, Aug. 2011, doi: 10.1108/13552541111156450.
[50] S. Hallmann, T. Wolny, and C. Emmelmann, "Post-processing of additively manufactured cutting edges by laser ablation," in *Procedia CIRP*, Jan. 2018, vol. 74, pp. 276–279, doi: 10.1016/j.procir.2018.08.110.
[51] A. Lalehpour, C. Janeteas, and A. Barari, "Surface roughness of FDM parts after post-processing with acetone vapor bath smoothing process," *Int. J. Adv. Manuf. Technol.*, vol. 95, no. 1–4, pp. 1505–1520, Mar. 2018, doi: 10.1007/s00170-017-1165-5.
[52] L. Blunt and X. Jiang, *Advanced Techniques for Assessment Surface Topography: Development of a Basis for 3D Surface Texture Standards "Surfstand."* Elsevier Inc., 2003.
[53] D. J. Whitehouse, "Surface metrology," *Meas. Sci. Technol.*, vol. 8, no. 9, pp. 955–972, 1997, doi: 10.1088/0957-0233/8/9/002.
[54] R. Leach, "Surface Texture," in *CIRP Encyclopedia of Production Engineering*, L. Laperrière and G. Reinhart, Eds. Springer Berlin Heidelberg, 2014, pp. 1–4.
[55] "ISO 25178-6:2010(en), Geometrical product specifications (GPS) — Surface texture: Areal — Part 6: Classification of methods for measuring surface texture." https://www.iso.org/obp/ui#iso:std:iso:25178:-6:ed-1:v1:en:biblref:13 (accessed Aug. 05, 2020).
[56] R. Leach, "Characterisation of areal surface texture," *Characterisation Areal Surf. Texture*, vol. 9783642364, pp. 1–353, 2013, doi: 10.1007/978-3-642-36458-7.
[57] "ISO 3274:1997, Geometrical Product Specifications (GPS) — Surface texture: Profile method — Nominal characteristics of contact (stylus) instruments." https://www.iso.org/obp/ui/#iso:std:iso:3274:ed-2:v1:en (accessed Aug. 07, 2020).
[58] K. Creath, "V Phase-Measurement Interferometry Techniques," *Prog. Opt.*, vol. 26, no. C, pp. 349–393, Jan. 1988, doi: 10.1016/S0079-6638(08)70178-1.
[59] G. E. Sommargren, "Optical heterodyne profilometry," *Appl. Opt.*, vol. 20, no. 4, p. 610, Feb. 1981, doi: 10.1364/ao.20.000610.
[60] J. M. Eastman and J. M. Zavislan, "A New Optical Surface Microprofiling Instrument," in *Precision Surface Metrology*, 1983, vol. 0429, pp. 56–64, doi: 10.1117/12.936340.
[61] T. Grimm, G. Wiora, and G. Witt, "Characterization of typical surface effects in additive manufacturing with confocal microscopy," *Surf. Topogr. Metrol. Prop.*, vol. 3, no. 1, p. 014001, Jan. 2015, doi: 10.1088/2051-672X/3/1/014001.
[62] L. Newton *et al.*, "Areal topography measurement of metal additive surfaces using focus variation microscopy," *Addit. Manuf.*, vol. 25, pp. 365–389, Jan. 2019, doi: 10.1016/j.addma.2018.11.013.
[63] A. V. Krishna, O. Flys, V. V Reddy, and B. G. Rosén, "Surface topography characterization using 3D stereoscopic reconstruction of SEM images," *Surf. Topogr. Metrol. Prop.*, vol. 6, no. 2, p. 024006, May 2018, doi: 10.1088/2051-672X/AABDE1.

[64] G. Ercolano *et al.*, “Additive manufacturing of sub-micron to sub-mm Metal structures with hollow AFM cantilevers,” *Micromachines*, vol. 11, no. 1, Jan. 2020, doi: 10.3390/mi11010006.
[65] “ASTM F1048 - 87(1999) Standard Test Method for Measuring the Effective Surface Roughness of Optical Components by Total Integrated Scattering (Withdrawn 2003).” www.astm.org (accessed Aug. 28, 2020).
[66] J. M. Bennett and L. Mattsson, *Introduction to Surface Roughness and Scattering*. Optical Society of America, 1989.
[67] B. J. N, F. R. E, and S. L. Y, “A capacitance-based surface texture measuring system.,” *CIRP Ann*, vol. 26, no. 1, pp. 375–377, 1977, Accessed: Aug. 28, 2020. [Online]. Available: https://jglobal.jst.go.jp/en/detail?JGLOBAL_ID=201002027345082954.
[68] A. M. Hamouda, “A precise pneumatic co-axial jet gauging system for surface roughness measurements,” *Precis. Eng.*, vol. 1, no. 2, pp. 95–100, Apr. 1979, doi: 10.1016/0141-6359(79)90140-5.
[69] V. Radhakrishnan, “Effect of stylus radius on the roughness values measured with tracing stylus instruments,” *Wear*, vol. 16, no. 5, pp. 325–335, Nov. 1970, doi: 10.1016/0043-1648(70)90099-2.
[70] M. Piska and J. Metelkova, “On the comparison of contact and non-contact evaluations of a machined surface,” *MM Sci. J.*, no. June 2014, pp. 476–479, 2014, doi: 10.17973/mmsj.2014_06_201408.
[71] S. H. R. Ali, “Advanced Nanomeasuring Techniques for Surface Characterization,” *ISRN Opt.*, vol. 2012, pp. 1–23, 2012, doi: 10.5402/2012/859353.
[72] “ISO - ISO 25178-602:2010 - Geometrical product specifications (GPS) — Surface texture: Areal — Part 602: Nominal characteristics of non-contact (confocal chromatic probe) instruments.” https://www.iso.org/standard/43920.html (accessed Aug. 05, 2020).
[73] F. Cabanettes *et al.*, “Topography of as built surfaces generated in metal additive manufacturing: A multi scale analysis from form to roughness,” *Precis. Eng.*, vol. 52, pp. 249–265, Apr. 2018, doi: 10.1016/j.precisioneng.2018.01.002.
[74] C. Bermudez, A. Matilla, and A. Aguerri, “Confocal fusion: towards the universal optical 3D metrology technology,” in *EUSPEN - LAMDAMAP*, 2017.
[75] A. Matilla, J. Mariné, J. Pérez, C. Cadevall, and R. Artigas, “Three-dimensional measurements with a novel technique combination of confocal and focus variation with a simultaneous scan,” in *Proceedings of the 16th International Conference of the European Society for Precision Engineering and Nanotechnology, EUSPEN 2016*, Apr. 2016, vol. 9890, p. 98900B, doi: 10.1117/12.2227054.
[76] O. Flys, J. Berglund, and B. G. Rosen, “Using confocal fusion for measurement of metal AM surface texture,” *Surf. Topogr. Metrol. Prop.*, vol. 8, no. 2, 2020, doi: 10.1088/2051-672X/ab84c3.
[77] “ISO 25178-2:2012(en), Geometrical product specifications (GPS) — Surface texture: Areal — Part 2: Terms, definitions and surface texture parameters.” https://www.iso.org/obp/ui/#iso:std:iso:25178:-2:ed-1:v1:en (accessed Aug. 09, 2020).
[78] F. Blateyron and A. Caulcutt, “3D Imaging and Analysis,” *Imaging Microsc.*, vol. 8, no. 3, pp. 42–43, 2006, doi: 10.1002/imic.200790094.
[79] “ISO 16610-1:2015(en), Geometrical product specifications (GPS) — Filtration — Part 1: Overview and basic concepts.” https://www.iso.org/obp/ui/#iso:std:iso:16610:-1:ed-1:v1:en (accessed Aug. 07, 2020).
[80] O. Flys, “On surface structure characterization and application on additive manufacturing,” 2020, Accessed: Aug. 07, 2020. [Online]. Available:

https://research.chalmers.se/en/publication/516839.
[81] “ISO 4288:1996(en), Geometrical Product Specifications (GPS) — Surface texture: Profile method — Rules and procedures for the assessment of surface texture.” https://www.iso.org/obp/ui/#iso:std:iso:4288:ed-2:v1:en:sec:B (accessed Aug. 09, 2020).
[82] “ISO 16610-21:2011(en), Geometrical product specifications (GPS) — Filtration — Part 21: Linear profile filters: Gaussian filters.” https://www.iso.org/obp/ui/#iso:std:iso:16610:-21:ed-1:v1:en (accessed Aug. 09, 2020).
[83] “Profile parameters from ISO 4287 - Surface Metrology Guide - Digital Surf.” https://guide.digitalsurf.com/en/guide-iso-4287-parameters.html (accessed Aug. 09, 2020).
[84] T. R. Thomas, *Rough Surfaces*. PUBLISHED BY IMPERIAL COLLEGE PRESS AND DISTRIBUTED BY WORLD SCIENTIFIC PUBLISHING CO., 1998.
[85] “ISO 4287:1997(en,fr), Geometrical Product Specifications (GPS) — Surface texture: Profile method — Terms, definitions and surface texture parameters / Spécification géométrique des produits (GPS) — État de surface: Méthode du profil — Termes, définitions et paramètres d’état de surface.” https://www.iso.org/obp/ui#iso:std:iso:4287:ed-1:v1:en,fr (accessed Aug. 05, 2020).
[86] M. C. Salcedo, I. B. Coral, and G. V. Ochoa, “Characterization of Surface Topography with Abbott Firestone Curve,” *Contemp. Eng. Sci.*, vol. 11, no. 68, pp. 3397–3407, 2018, doi: 10.12988/ces.2018.87319.
[87] F. Blateyron, “Stratified Surface,” in *CIRP Encyclopedia of Production Engineering*, Springer Berlin Heidelberg, 2018, pp. 1–7.
[88] ASME, *B46.1:2002 Surface Texture (Surface Roughness, Waviness, and Lay) - ASME*. 2002.
[89] R. N. Youngworth, B. B. Gallagher, and B. L. Stamper, “An overview of power spectral density (PSD) calculations,” *Opt. Manuf. Test. VI*, vol. 5869, no. August 2005, p. 58690U, 2005, doi: 10.1117/12.618478.
[90] E. Sidick, “Power spectral density specification and analysis of large optical surfaces,” *Model. Asp. Opt. Metrol. II*, vol. 7390, no. June 2009, p. 73900L, 2009, doi: 10.1117/12.823844.
[91] T. D. B. Jacobs, T. Junge, and L. Pastewka, “Quantitative characterization of surface topography using spectral analysis,” *Surf. Topogr. Metrol. Prop.*, vol. 5, no. 1, 2017, doi: 10.1088/2051-672X/aa51f8.
[92] C. A. Brown, “Areal fractal methods,” in *Characterisation of Areal Surface Texture*, vol. 9783642364587, Springer-Verlag Berlin Heidelberg, 2013, pp. 129–153.
[93] C. A. Brown, W. A. Johnsen, R. M. Butland, and J. Bryan, “Scale-Sensitive Fractal Analysis of Turned Surfaces,” *CIRP Ann. - Manuf. Technol.*, vol. 45, no. 1, pp. 515–518, Jan. 1996, doi: 10.1016/S0007-8506(07)63114-X.
[94] J. Berglund, *Characterisation of Functional Pressing Die Surfaces*. Chalmers University of Technology, 2011.
[95] C. A. Brown *et al.*, “Multiscale analyses and characterizations of surface topographies,” *CIRP Ann.*, vol. 67, no. 2, pp. 839–862, Jan. 2018, doi: 10.1016/j.cirp.2018.06.001.
[96] N. Senin, A. Thompson, and R. Leach, “Feature-based characterisation of signature topography in laser powder bed fusion of metals,” *Meas. Sci. Technol.*, vol. 29, no. 4, p. 045009, Mar. 2018, doi: 10.1088/1361-6501/aa9e19.
[97] S. Lou, W. Zeng, L. Pagani, H. Abdul-Rahman, X. Jiang, and P. J. Scott,

"Development of Surface Characterisation Toolbox for Additive Manufactured Components: from Planar Layer Surfaces to Complex Functional Surfaces." Accessed: Aug. 17, 2020. [Online]. Available: www.euspen.eu.
[98] A. Boschetto, L. Bottini, and F. Veniali, "Roughness modeling of AlSi10Mg parts fabricated by selective laser melting," *J. Mater. Process. Technol.*, vol. 241, pp. 154–163, Mar. 2017, doi: 10.1016/j.jmatprotec.2016.11.013.
[99] B. G. Rosen, A. Fall, S. Rosen, A. Farbrot, and P. Bergström, "Topographic modelling of haptic properties of tissue products," in *Journal of Physics: Conference Series*, 2014, vol. 483, no. 1, doi: 10.1088/1742-6596/483/1/012010.
[100] S. Chatterjee and J. S. Simonoff, *Handbook of Regression Analysis*. Somerset, UNITED STATES: John Wiley & Sons, Incorporated, 2012.
[101] J. Berglund and B. G. Rosén, "A method development for correlation of surface finish appearance of die surfaces and roughness measurement data," *Tribol. Lett.*, vol. 36, no. 2, pp. 157–164, Nov. 2009, doi: 10.1007/s11249-009-9470-2.
[102] "ISO/ASTM 52902:2019(en), Additive manufacturing — Test artifacts — Geometric capability assessment of additive manufacturing systems." https://www.iso.org/obp/ui/#iso:std:iso-astm:52902:ed-1:v1:en (accessed Aug. 09, 2020).
[103] P. Reeves and R. Cobb, "Surface deviation modeling of LMT Processes–a comparative analysis," *Proc. Fifth Eur. Conf. Rapid Prototyp. Manuf.*, Jun. 1995.
[104] A. K. Sood, R. K. Ohdar, and S. S. Mahapatra, "Improving dimensional accuracy of Fused Deposition Modelling processed part using grey Taguchi method," *Mater. Des.*, vol. 30, no. 10, pp. 4243–4252, Dec. 2009, doi: 10.1016/j.matdes.2009.04.030.